

AD A101602

HDL-CR-81-723-1

May 1981

Performance Calculations and  
Optimization of Gas Guns

Prepared by

Arnold E. Selgel  
3302 Pauline Drive  
Chevy Chase, MD 20015

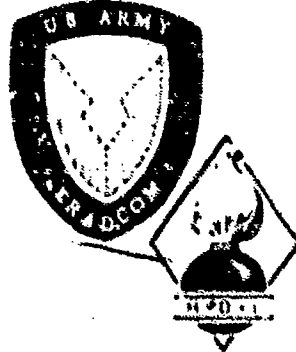
Under contract

DAAG39-76/M-723

LEVEL II

12

DTIC  
ELECTED  
JUN 23 1981  
S E D



U.S. Army Electronics Research  
and Development Command  
Harry Diamond Laboratories  
Adelphi, MD 20783

FILE COPY

Approved for public release; distribution unlimited.

~~New~~ 412442

81 6 23 006

The findings in this report are not to be construed as an official Department of the Army position unless so designated by other authorized documents.

Citation of manufacturers' or trade names does not constitute an official endorsement or approval of the use thereof.

Destroy this report when it is no longer needed. Do not return it to the originator.

## UNCLASSIFIED

SECURITY CLASSIFICATION OF THIS PAGE (When Data Entered)

49 REPORT DOCUMENTATION PAGE		READ INSTRUCTIONS BEFORE COMPLETING FORM	
1. REPORT NUMBER HDL-CR-81-723-1	2. GOVT ACCESSION NO. AD-A101 602	3. RECIPIENT'S CATALOG NUMBER 9	
4. TITLE (INCLUDE SUBTITLE) Performance Calculations and Optimization of Gas Guns		5. TYPE OF REPORT & PERIOD COVERED Contractor's Report	
6. PERFORMING ORG. REPORT NUMBER		7. CONTRACT OR GRANT NUMBER(S) DAAG39-76-M-723	
8. PERFORMING ORGANIZATION NAME AND ADDRESS 3302 Pauline Drive Chevy Chase, MD 20015		10. PROGRAM ELEMENT, PROJECT, TASK AREA & WORK UNIT NUMBERS Program Element 6.21.20.A	
11. CONTROLLING OFFICE NAME AND ADDRESS Harry Diamond Laboratories 2800 Powder Mill Road Adelphi, Maryland 20783		12. REPORT DATE May 1981	13. NUMBER OF PAGES 45
14. MONITORING AGENCY NAME & ADDRESS (if different from Controlling Office)		15. SECURITY CLASS. (of this report) Unclassified	
16. DISTRIBUTION STATEMENT (of this Report) Approved for public release; distribution unlimited		17. DECLASSIFICATION/DOWNGRADING SCHEDULE	
18. DISTRIBUTION STATEMENT (of the abstract entered in Block 10, if different from Report) Approved for public release; distribution unlimited			
19. SUPPLEMENTARY NOTES HDL Project: A77886 ORCMS Code: 612120.H250011 DA Project: 11162120AH2501			
20. KEY WORDS (Continue on reverse side if necessary and identify by block number)			
21. ABSTRACT (Continue on reverse side if necessary and identify by block number) Compressed gas guns are used at the Harry Diamond Laboratories (HDL) to test fuzes and fuze components. Calculations were made to describe the performance of both existing HDL gas guns and planned future HDL gas guns. In the latter case, chamber diameter and chamber length were varied to evaluate their effect on projectile velocity. These results permit selection of an optimum chamber geometry.			

DD FORM 1 JAN 73 EDITION OF 1 NOV 68 IS OBSOLETE

UNCLASSIFIED

SECURITY CLASSIFICATION OF THIS PAGE (When Data Entered)

412442

## CONTENTS

	<u>Page</u>
NOMENCLATURE . . . . .	5
1. INTRODUCTION . . . . .	7
1.1 Use of Gas Guns at Harry Diamond Laboratories. . . . .	7
1.2 Preburned Propellant Gun . . . . .	7
2. CALCULATIONS ON HDL GAS GUNS . . . . .	8
2.1 Assumptions Made in Calculations . . . . .	9
2.2 Methods Used to Calculate Gas Gun Performance. . . . .	9
3. RESULTS OF CALCULATIONS. . . . .	10
3.1 Existing HDL Guns. . . . .	10
3.2 Future HDL Guns. . . . .	10
3.3 Effects which Decrease Projectile Velocity . . . . .	17
Appendix A. Description of the Preburned Propellant Gun . . . . .	29
Appendix B. The Gas Dynamics Equations for a Chambered Propellant Gas Gun . . . . .	31
Appendix C. Calculations by Electronic Computing Machines . . . . .	37
Appendix D. The Special Solution of Pidduck-Kent. . . . .	39
DISTRIBUTION . . . . .	45

## ILLUSTRATIONS

<u>Figure</u>		<u>Page</u>
1	HDL Preburned Propellant Gas Gun. . . . .	7
2	HDL Gas Gun . . . . .	7
3	2-Inch Gun, Air Driven. . . . .	11
4	2-Inch Gun, Helium Driven . . . . .	11
5	Comparison of Air and Helium Drivers for 2-Inch Gun . . . . .	12
6	Velocity as Function of Breech Position for Fixed Length (3-Inch) Air Driven Gun . . . . .	12
7	Velocity as Function of Breech Position for Fixed Length (3-Inch) Helium Driven Gun. . . . .	13
8	Comparison of Air and Helium Drivers for Variable Breech Position in Fixed Length 3-Inch Gun . . . . .	13
9	Velocity as Function of Breech Position for Fixed Length (4-Inch) Nitrogen Driven Gun. . . . .	14
10	Velocity as Function of Breech Position for Fixed Length (4-Inch) Helium Driven Gun. . . . .	14
11	Effect of Chambrage on 4-Inch Nitrogen Driven Gun . . . . .	15

## CONTENTS (cont.)

<u>Figure</u>		<u>Page</u>
12	Expected Characteristics of 7-Inch Infinite Reservoir Gun . . . . .	16
13	Predicted Performance of 7-Inch Gun with 100-Foot Driver Section . . . . .	16
14	Velocity as Function of Breech Position for Fixed Length 3-Inch and 9-Inch Launchers . . . . .	18
15	Velocity as Function of Breech Position for Fixed Length Air Gun, $D_o/D_1 = 1$ . . . . .	19
16	Velocity as Function of Breech Position for Fixed Length Air Gun, $D_o/D_1 = 2$ . . . . .	19
17	Velocity as Function of Breech Position for Fixed Length Air Gun, Max Acceleration = 320 g. . . . .	20
18	Velocity as Function of Breech Position for Fixed Length Air Gun, Max Acceleration = 1280 g. . . . .	20
19	Velocity as Function of Breech Position for Fixed Length Air Gun, Max Acceleration = 3200 g. . . . .	21
20	Velocity as Function of Breech Position for Fixed Length Helium Gun, $D_o/D_1 = 1$ . . . . .	22
21	Velocity as Function of Breech Position for Fixed Length Helium Gun, $D_o/D_1 = 2$ . . . . .	22
22	Velocity as Function of Breech Position for Fixed Length Helium Gun, Max Acceleration = 320 g . . . . .	23
23	Velocity as Function of Breech Position for Fixed Length Helium Gun, Max Acceleration = 1200 g. . . . .	23
24	Velocity as Function of Breech Position for Fixed Length Helium Gun, Max Acceleration = 3200 g . . . . .	24
25	Velocity as Function of Breech Position for Fixed Length Gas Guns, Max Acceleration = 320 g. . . . .	25
26	Velocity as Function of Breech Position for Fixed Length Gas Guns, Max Acceleration = 1280 g . . . . .	25
27	Velocity as Function of Breech Position for Fixed Length Gas Guns, Max Acceleration = 3200 g . . . . .	26
<u>Table</u>		
I	Existing HDL Gas Guns . . . . .	8
II	Future HDL Gas Guns . . . . .	9

## NOMENCLATURE

a	Sound speed of driver gas.
A	Local gun cross-sectional area.
b	Covolume.
D	Inside diameter.
E	Internal energy of driver gas in control volume.
g	Initial (maximum) projectile acceleration.
G	Mass of driver gas initially in reservoir.
h	Enthalpy of driver gas.
L	Gun barrel length.
m	Mass of driver gas in control volume.
M	Projectile mass.
n	Arbitrary integer.
N	Degrees of freedom of driver gas.
P	Gas pressure.
R	Gas constant.
t	Time.
T	Gas temperature.
u	Gas Velocity.
$u_p$	Projectile Mach number based on initial gas sound speed ( $u_p/a_0$ ).
v	Specific volume.
x	Dimensional position coordinate along gun axis.
$x_p$	Nondimensional gun barrel length ( $x_p A_0 L / Ma_0^2$ ).
Z	Fractional pin position in gun. $[x_0 / (x_0 + L)]$
a	Parameter of Pidduck Kent solution.
$\gamma$	Driver gas adiabatic constant (5/3 for helium; 7/5 for air and nitrogen).
$\rho$	Local instantaneous driver gas density.
$\rho_0$	Initial gas density in reservoir.
c	Riemann function of driver gas.

### Subscripts

c Control volume.  
 0, o Initial state in chamber at gun.  
 i Position in barrel at exit of transition section.  
 l Gas barrel.  
 p Projectile.

RE: Contract DAAG-39-76-N-723

There should be four digits at end of contract but contract office at HDL unable to verify. The records have been retired per Ms. Dydak, contract office and Mr. Curshack, project officer

## 1. INTRODUCTION

### 1.1 Use of Gas Guns at Harry Diamond Laboratories

Gas guns are used at the Harry Diamond Laboratories (HDL) to accelerate ordnance items to velocities typical of artillery projectiles, i.e., 500 to 4000 ft/s.

For certain test considerations, it is necessary to achieve the required velocity with a limited acceleration or g force exerted on the projectile while in the gun. Therefore, long barreled guns operating at low pressures are used. These guns are located in fixed length rooms. The characteristics of the guns must be known to configure them properly and to maximize the achievable velocity imparted to the fuze or fuze component for a particular acceleration level.

### 1.2 Preburned Propellant Gun

The gas guns at HDL are classed as preburned propellant (PP) guns. PP guns are described in appendix A. Schematically, they appear as sketched in figure 4. (See Nomenclature page for meanings of symbols.)

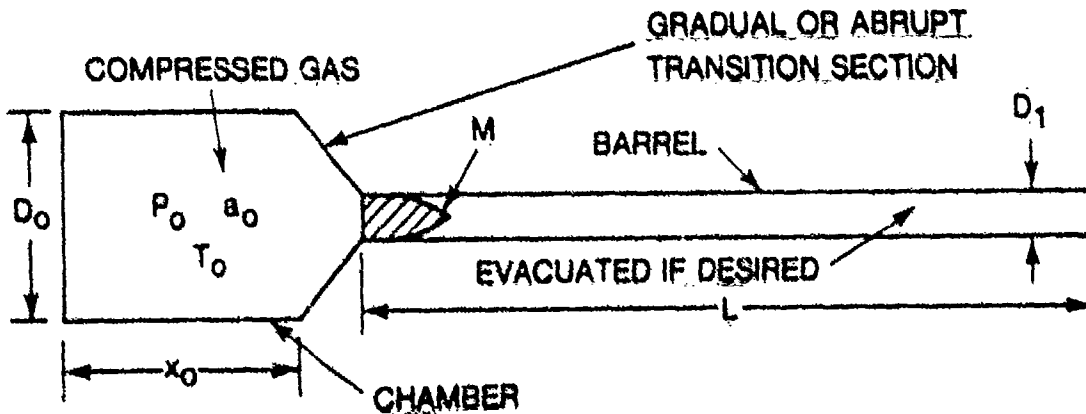


Figure 1. HDL Preburned Propellant Gas Gun.

In the HDL gas gun, the compressed gas (nitrogen, air, or helium) is at room temperature ( $T_0 \approx 20^\circ\text{C}$ ); one type of PP gun used at HDL is shown in figure 2.

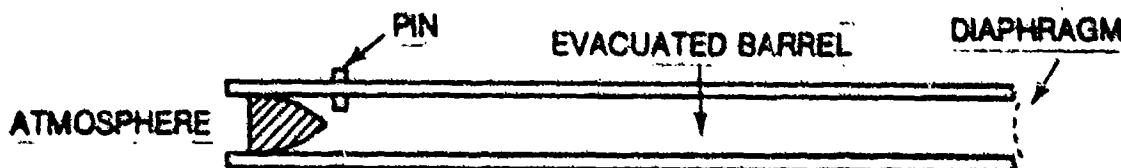


Figure 2. HDL Gas Gun.

## 2. CALCULATIONS ON HDL GAS GUNS

Specifically, two tasks were undertaken. One was the calculation of the performance of various configurations of four existing HDL gas guns. These guns have inside barrel diameters of 2, 3, 4, and 7 in. Table I lists data pertaining to these existing HDL gas guns.

TABLE I. EXISTING HDL GAS GUNS

Barrel		Chamber		Projectile		Propelling gas*	
D <sub>1</sub> (in.)	L + x <sub>0</sub> (ft) <sup>0</sup>	D (in. <sup>0</sup> )	x <sub>0</sub> (ft) <sup>0</sup>	M (gm)	Type	Max P (psi) <sup>0</sup>	
2	32		3.2 ft <sup>3</sup>	300 to 1000	Helium or air	100	
2	32	2	Infinite**	300 to 1000	Air	14.7	
3	97	3	20	1000 to 2000	Helium or air	600	
4	100	4	12, 24, or 36	400 to 3000	Helium or air	600	
7	100 or 314	7	Infinite**	400 to 10,000	Air	14.7	
7	314	7	100***	400 to 10,000	Helium or air	100	

\*T<sub>0</sub> = room temperature.

\*\*Projectile initially positioned at beginning of barrel with back of projectile subjected to atmosphere.

\*\*\*Possible configuration.

The second task was the calculation of the performance of and optimization of two future planned HDL gas guns. One gun will have a 3-in. inside barrel diameter; the other will have a 9-in. inside barrel diameter. Table II lists data pertaining to these future HDL gas guns.

TABLE II. FUTURE HDL GAS GUNS

Overall length ( $L + x_0$ ) (ft)	Barrel $D_1$ (in.)	Chamber $D_0$	Max acceleration	Max $P_0/M$ based on max acceleration	Propelling gas
200	3	To be optimized	3200 g	1 psi/gm	Helium or air
200	9	To be optimized	3200 g	9 psi/gm	Helium or air

### 2.1 Assumptions Made in Calculations

The following assumptions were made in the calculations:

- (1) The compressed propellant gas behaves as an ideal gas.
- (2) The compressed propellant gas expands isentropically.  
(Thus, gaseous frictional and heat-transfer effects are assumed negligible.)
- (3) Projectile friction is negligible.
- (4) There is no gas leakage around the projectile.
- (5) The pressure in front of the projectile is negligible.

These assumptions are discussed further in section 3.3.

### 2.2 Methods Used to Calculate Gas Gun Performance

The following two methods were used to calculate the performance of the HDL gas guns:

- (1) The plots that were used were dimensionless projectile velocity,  $u_p$ , versus nondimensional length,  $\bar{x}$ , plots.<sup>1</sup> They were obtained by applying the method of characteristics for the constant diameter chamber and the constant diameter barrel. Steady flow equations were used in the transition section. The calculations were done by electronic computing machines.

<sup>1</sup> A. E. Seigel, The Theory of High Speed Guns, Agardograph 91 (May 1965), obtainable from the National Technical Information Service, Defense Documentation Center, Springfield, VA, AD 475660.

The gas dynamics equations that were used are described in appendix B.

Additional information relative to the plots obtained from the electronic computers is discussed in appendix C.

(2) The second method used was the Pidduck-Kent Special Solution. This closed-form solution is an approximation to the wave solution. It is particularly accurate when applied to low G/M cases. (G is the gas mass, and M is the projectile mass.) This procedure was used to calculate performance in cases where the dimensionless  $\bar{u}_p$  versus  $\bar{x}$  plots were difficult to read and where G/M was less than 1/4. Appendix D describes the Pidduck-Kent Special Solution.

### 3. RESULTS OF CALCULATIONS

#### 3.1 Existing HDL Guns

The calculated results for the existing HDL guns are presented as plots in figures 3 to 13.

Figures 3 to 5 (2-in. gun) show projectile velocity ( $u_p$ ) as a function of initial pressure ( $P_0$ ), projectile mass (M), and type of gas (helium or air).

Figures 6 to 8 (3-in. gun) show the effects on projectile velocity of varying chamber length ( $x_0$ ), M, and gas (helium or air).

Figures 9 to 11 (4-in. gun) show the effects on projectile velocity of varying  $x_0$ , diameter ratio ( $D_0/D_1$ ), and gas (helium or air).

Finally, figures 12 and 13 show the effects on projectile velocity of varying M, length of barrel, and gas (helium or air).

#### 3.2 Future HDL Guns

The calculated results for the future HDL guns are presented as plots of  $u_p$  versus  $x_0$  in figures 14 to 27.

It was established here that the guns with 3- and 9-in.-diameter barrels could both be represented by the same  $u_p$  versus  $x_0$  plots because

$$\bar{u}_p = u_p/a_0 = \phi(\bar{x}_p, G/M, D_0/D_1, \text{given gas}).$$

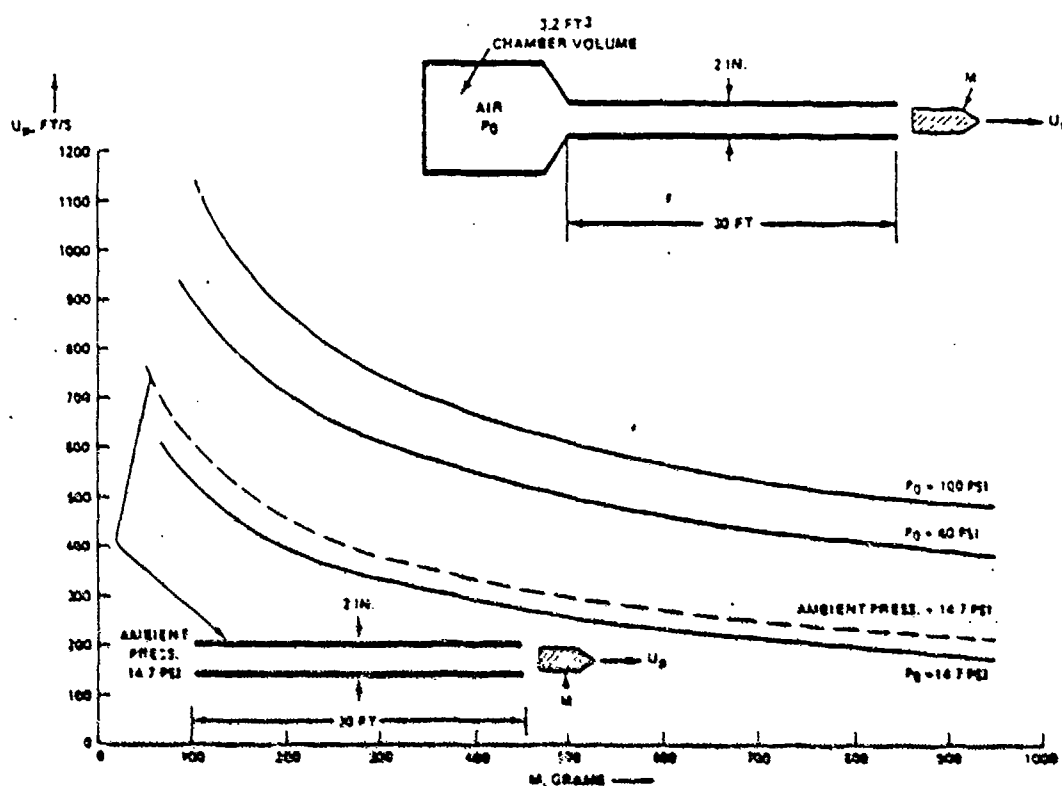


Figure 3. 2-Inch Gun; Air Driven

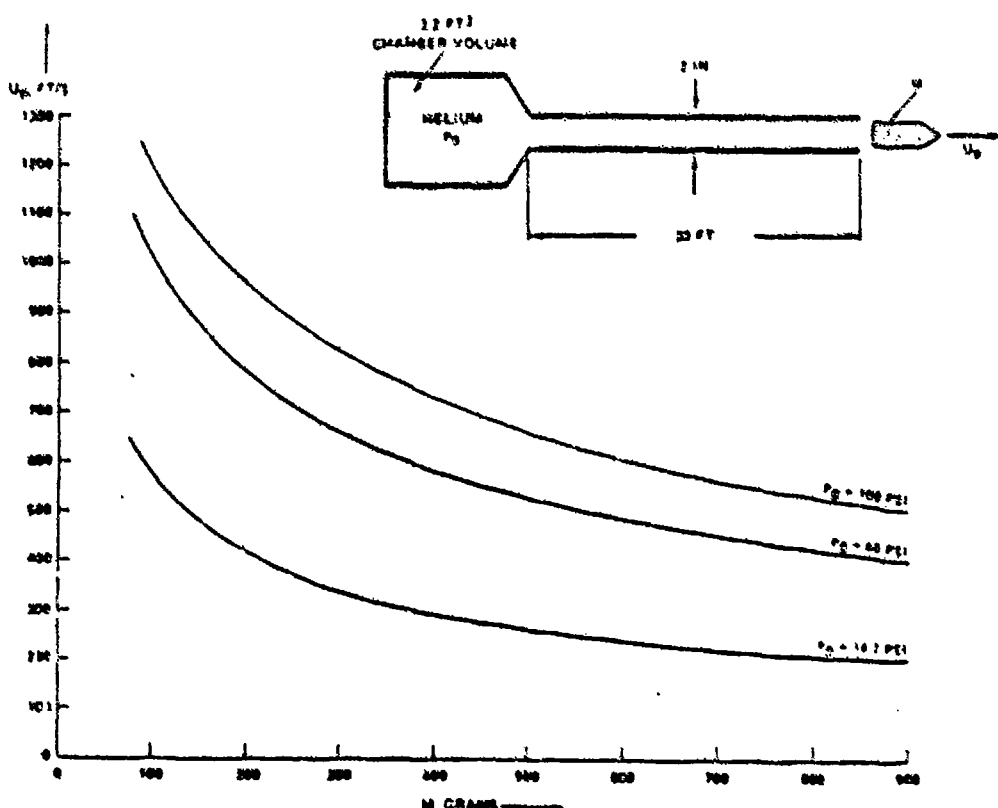


Figure 4. 2-Inch Gun; Helium Driven

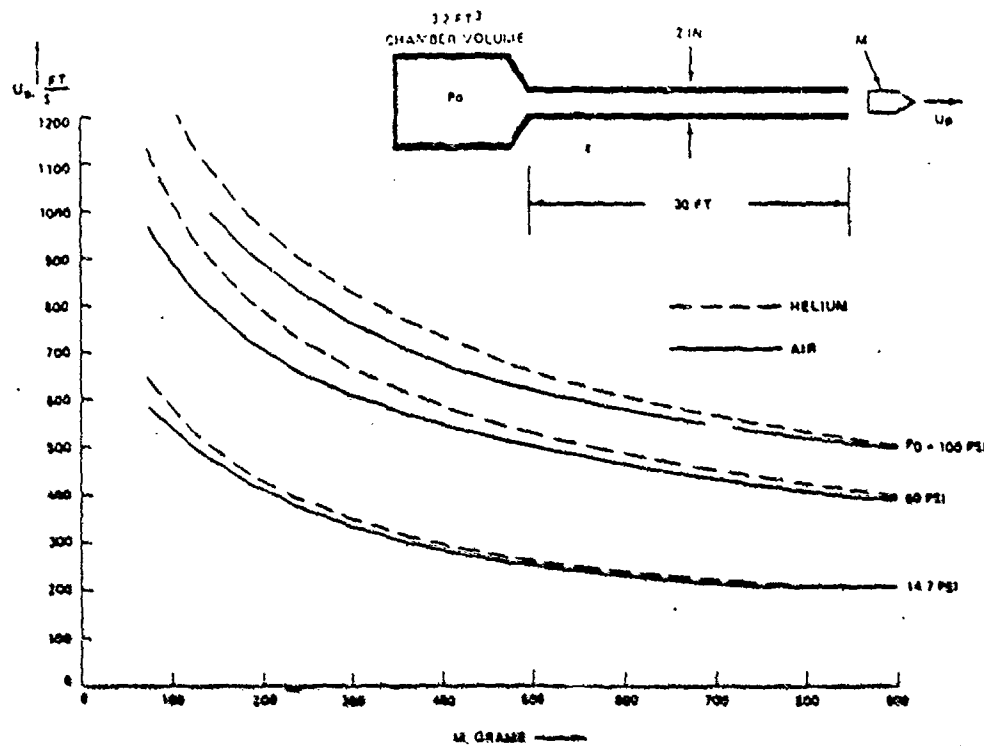


Figure 5. Comparison of Air and Helium Drivers for 2-Inch Gun

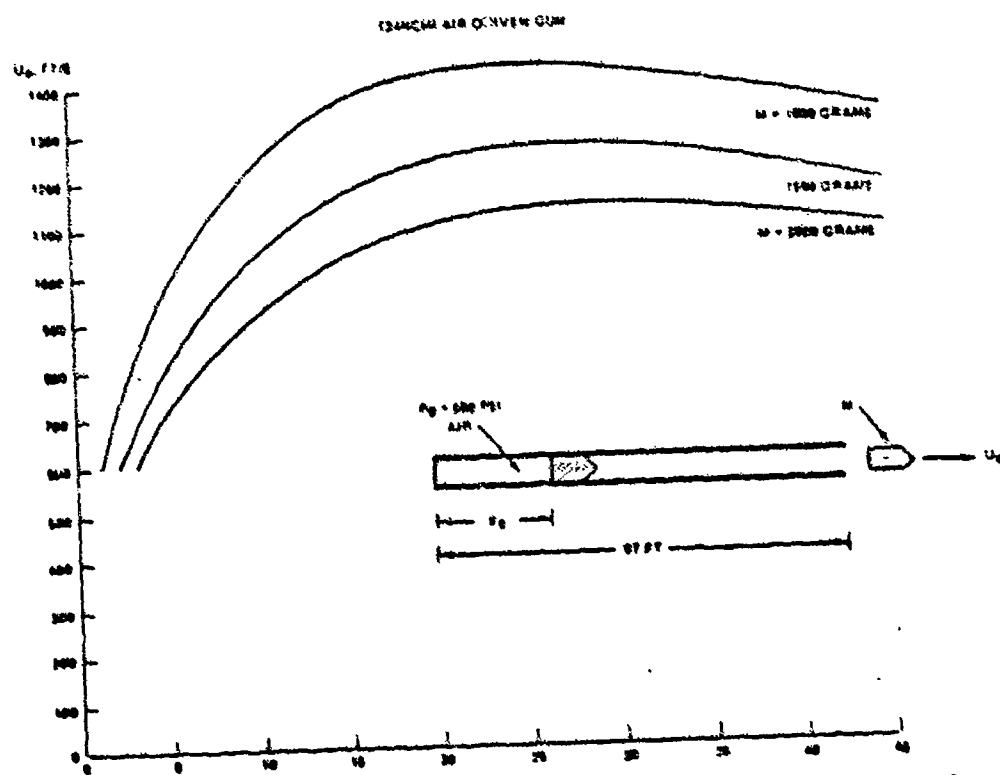


Figure 6. Velocity as Function of Breech Position for Fixed Length (3-Inch) Air Driven Gun

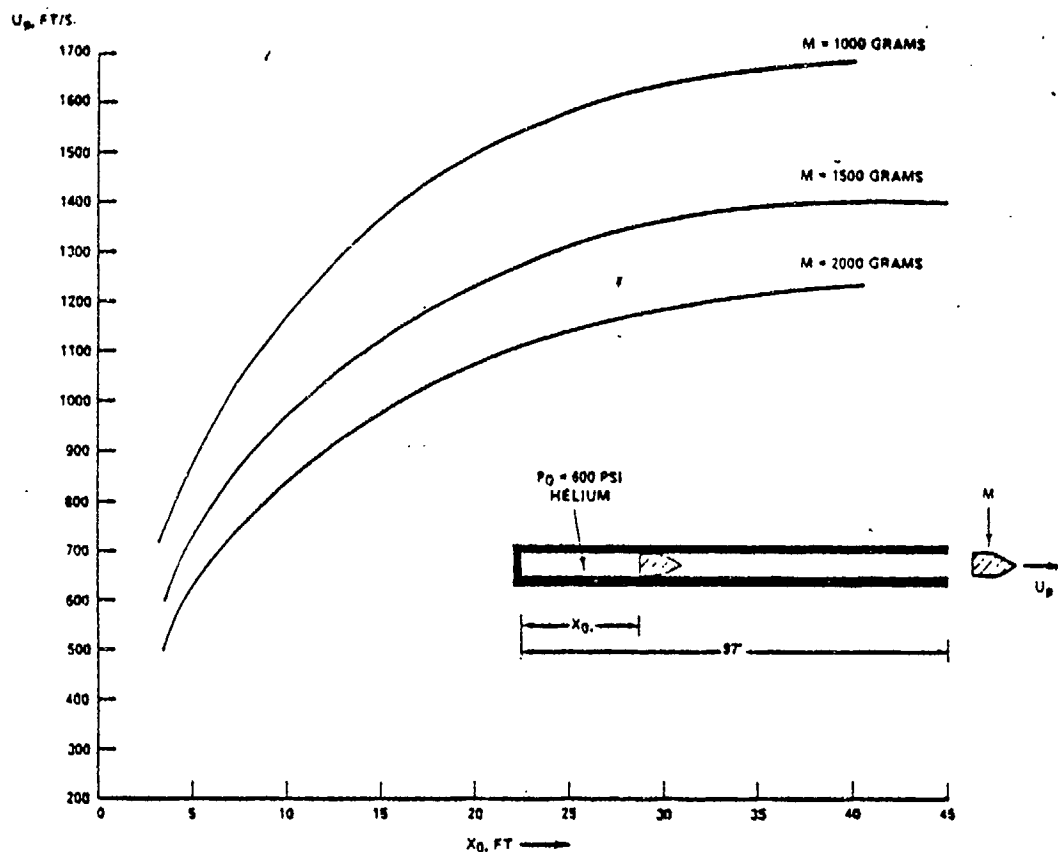


Figure 7. Velocity as Function of Breech Position for Fixed Length (3-Inch) Helium Driven Gun

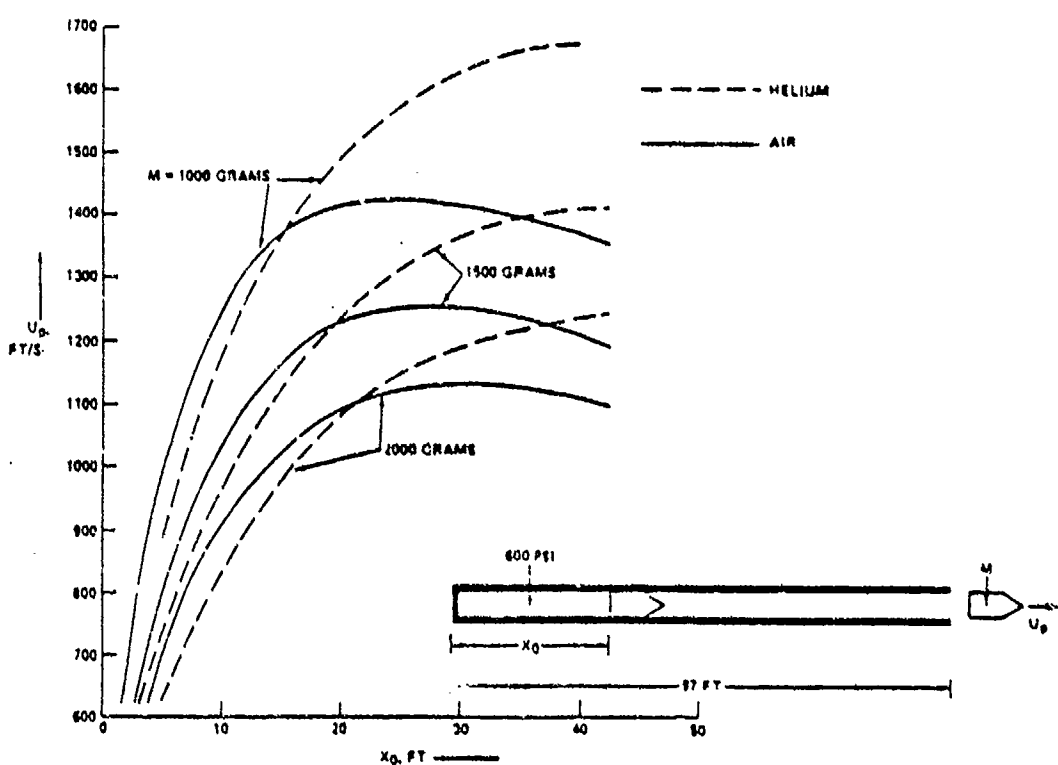


Figure 8. Comparison of Air and Helium Drivers for Variable Breech Position in Fixed Length 3-Inch Gun

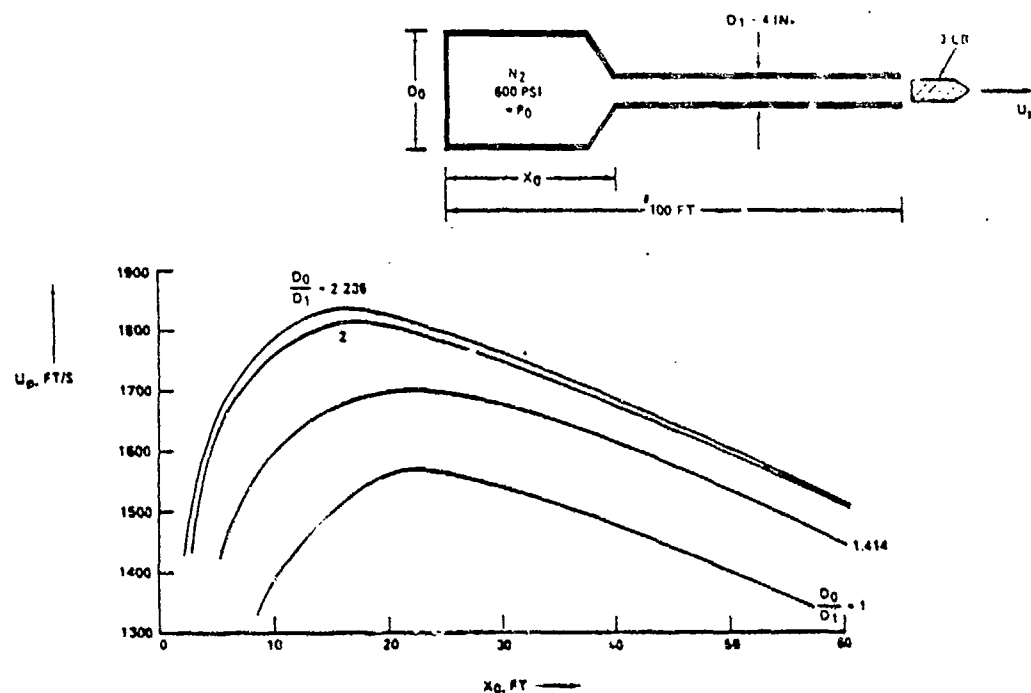


Figure 9. Velocity as Function of Breech Position for Fixed Length (4-Inch) Nitrogen Driven Gun

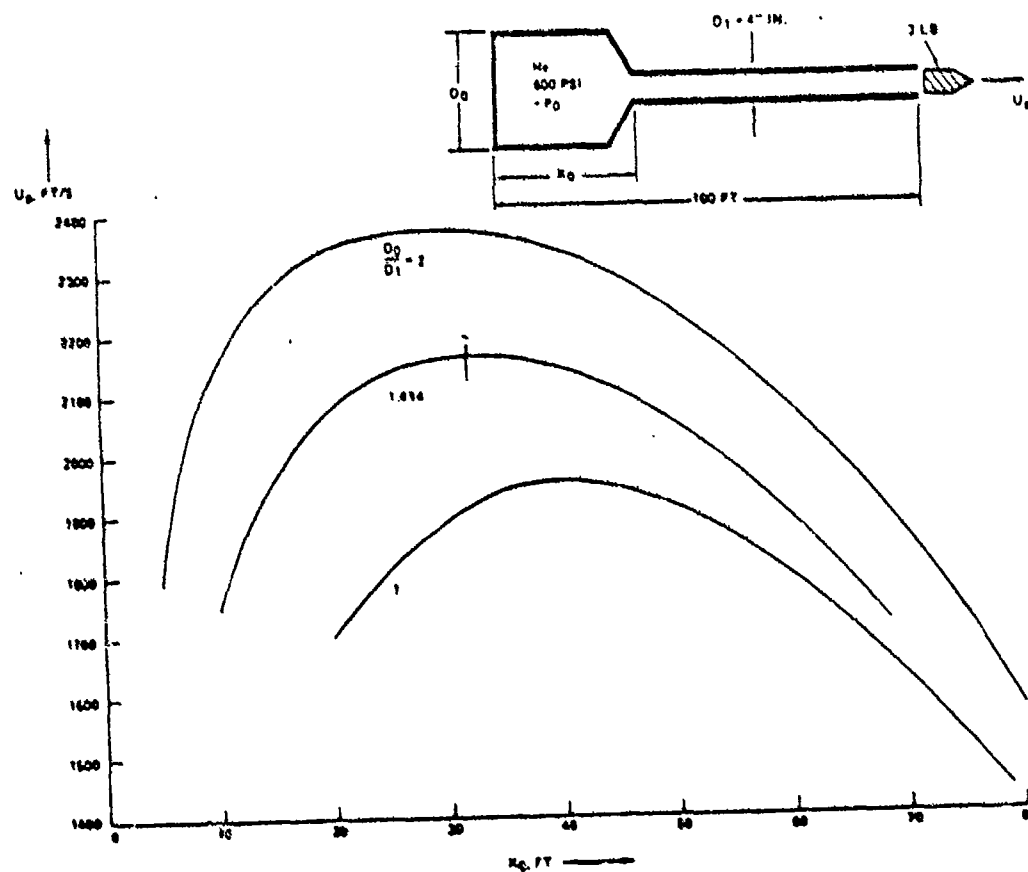


Figure 10. Velocity as Function of Breech Position for Fixed Length (4-Inch) Helium Driven Gun

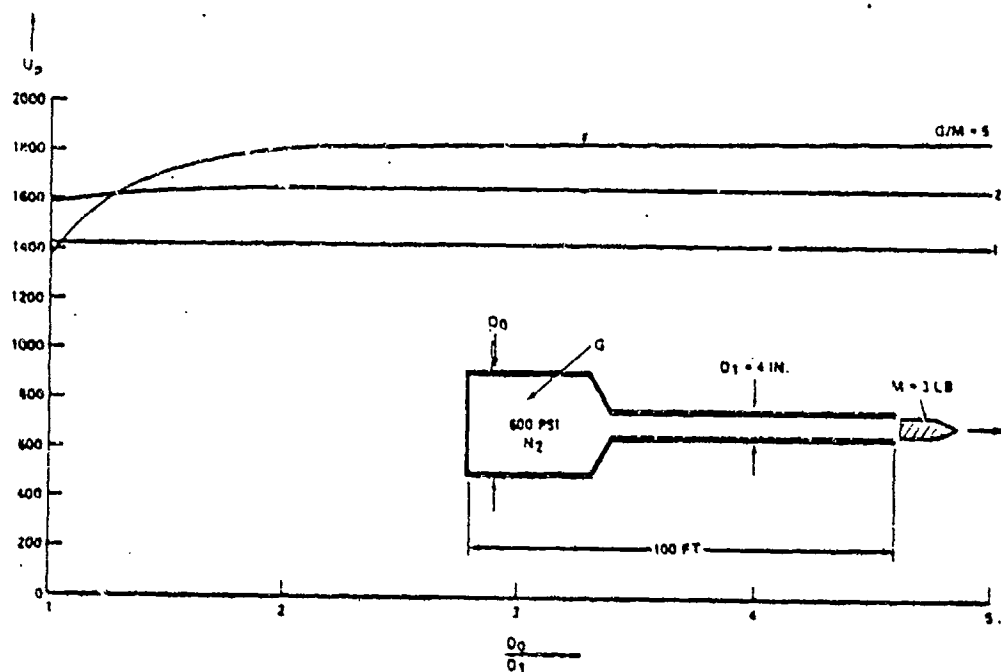


Figure 11. Effect of Chambrage (chamber) on 4-Inch Nitrogen Driven Gun

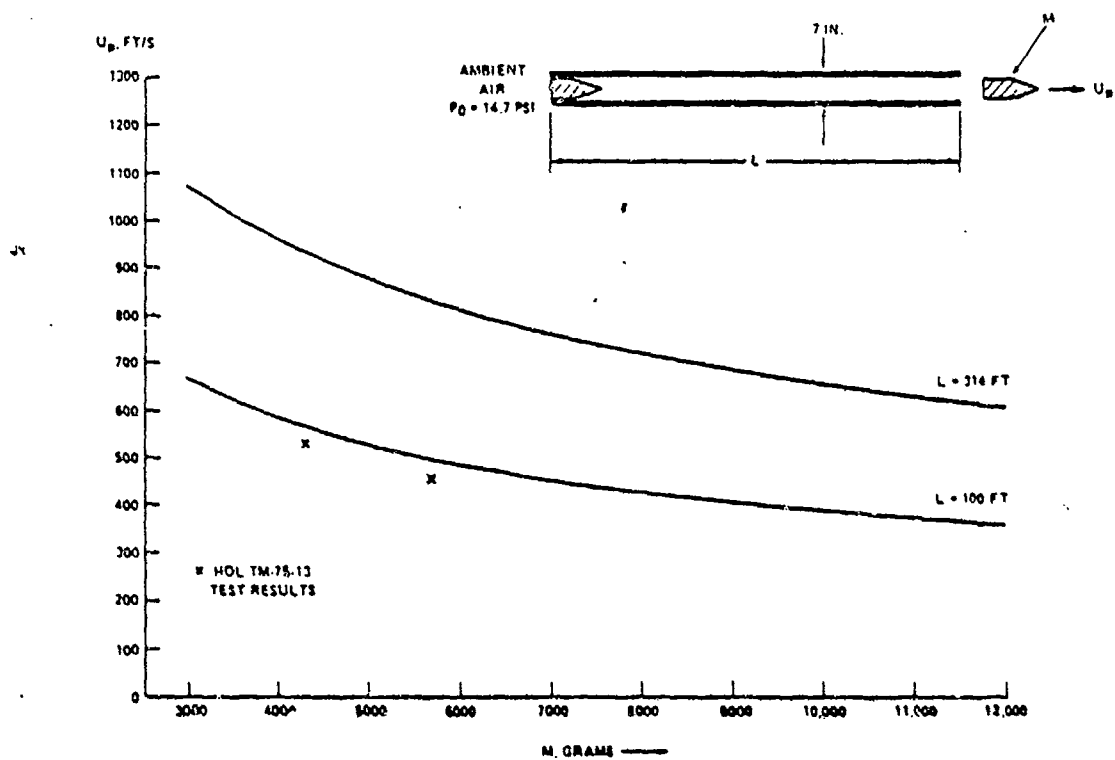


Figure 12. Expected characteristics of 7-Inch Infinite Reservoir Gun

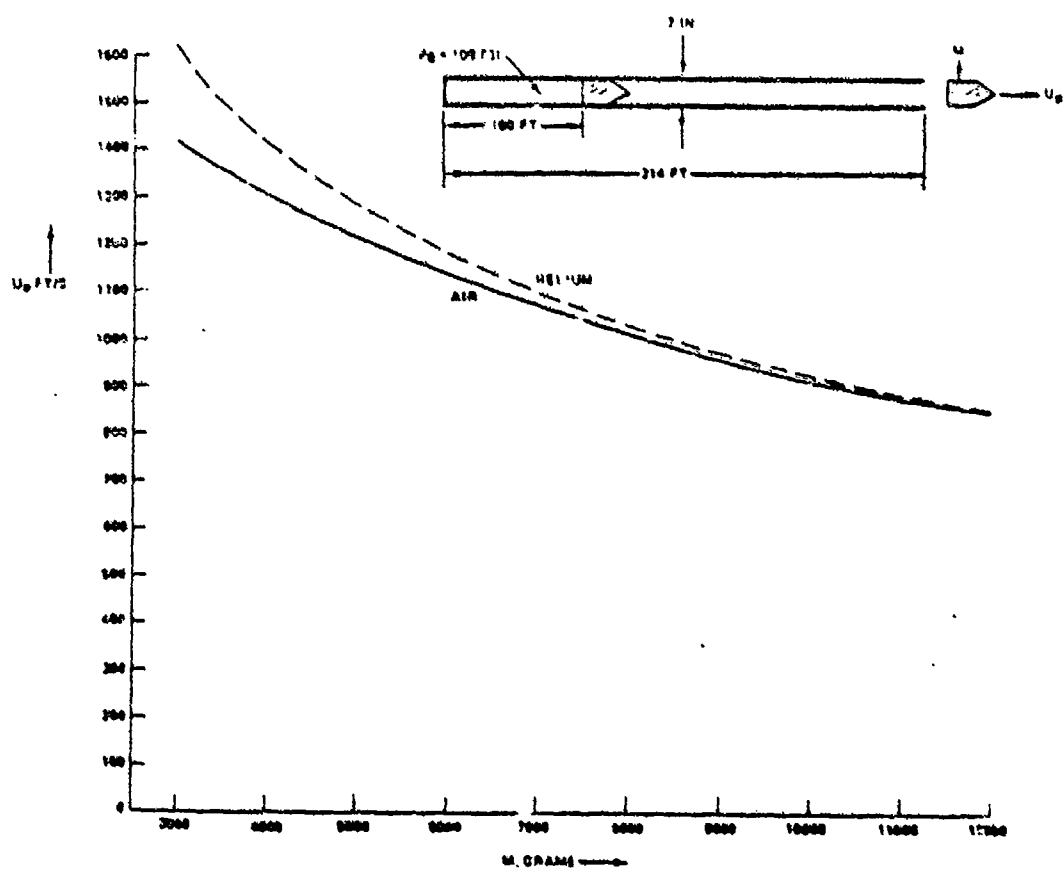


Figure 13. Predicted Performance of 7-Inch Gun with 100-Foot Driver Section

where

$$\bar{x}_p \equiv P_0 A_1 x_p / M a_0^2,$$

$$G/M = \rho_0 A_0 x_0 / M = (Y P_0 A_1 x_0 / M a_0^2) (D_0'/D_1).$$

Since the gun length, L, for both the 3- and 9-in. guns is 200 ft,

$$L = 200 - x_0.$$

Also, the acceleration may be expressed as

$$g = P_0 A_1 / M.$$

From the above equations, one obtains

$$u_p = u_p (g, x_0, D_0/D_1, \text{given gas}).$$

Thus, both the 3- and 9-in. guns are represented by the same plots for the case of equal g force.

Figure 14 shows a general arrangement of the 3- and 9-in. gas guns. This figure shows that three values for the maximum g force will be featured (3200, 1280 and 320 g).

Figures 15 to 19 are plots of  $u_p$  versus  $x_0$  for the three values of g force, varying  $D_0/D_1$ , and using compressed air as the propelling gas. Figures 20 to 24 are similar plots using compressed helium.

Figures 25 to 27 compare results obtained for compressed air and helium by showing  $u_p$  versus  $x_0$  for varying  $D_0/D_1$  ratios for the three g values.

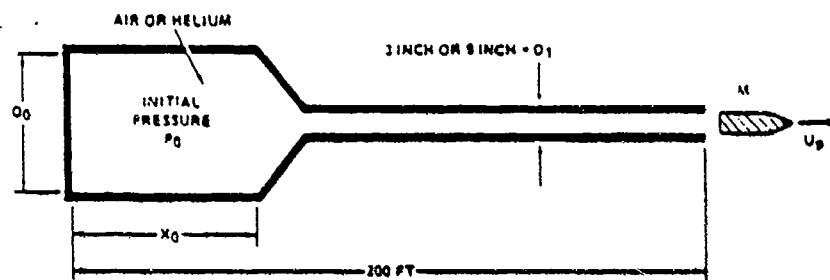
From the plots in these figures one may optimize the performance of the 3- and 9-in. gas guns by proper selection of the gun geometry. For example, from figure 27, if maximum velocity were desired at a maximum acceleration of 3200 g, one would design a gun with a  $D_0/D_1 = 2$  and  $x_0 = 30$  ft or so. One should check to make certain that the quantity of gas emerging from the barrel behind the projectile would not interfere with the experimental setup and could be taken care of safely.

### 3.3 Effects which Decrease Projectile Velocity

In the calculations, these were assumed:

(1) The compressed propellant gas is an ideal gas. Actually, the gas behavior is nonideal; as a result, the projectile velocity will be less than calculated, as has been demonstrated.<sup>1</sup> Nevertheless, the exact equation of state could be used to obtain the correct projectile velocity.

<sup>1</sup> A. E. Seigel, The Theory of High Speed Guns, Agardograph 91 (May 1965), obtainable from the National Technical Information Service, Defense Documentation Center, Springfield, VA, AD 475660.



MAXIMUM ACCELERATION $\cdot \frac{P0A1}{M}$	MAXIMUM ACCELERATION FOR EACH DIAMETER IN UNITS OF $\frac{P1}{GRAM}$ (EQUAL TO $\frac{P2}{M}$ )	
INCH	01 = ?'	01 = ?'
2200 g	1 PS/GRAM	9 PS/GRAM
1200 g	0.6 PS/GRAM	3.6 PS/GRAM
320 g	0.1 PS/GRAM	0.9 PS/GRAM

Figure 14. Velocity as Function of Breech Position for Fixed Length  
3-Inch and 9-Inch Launchers

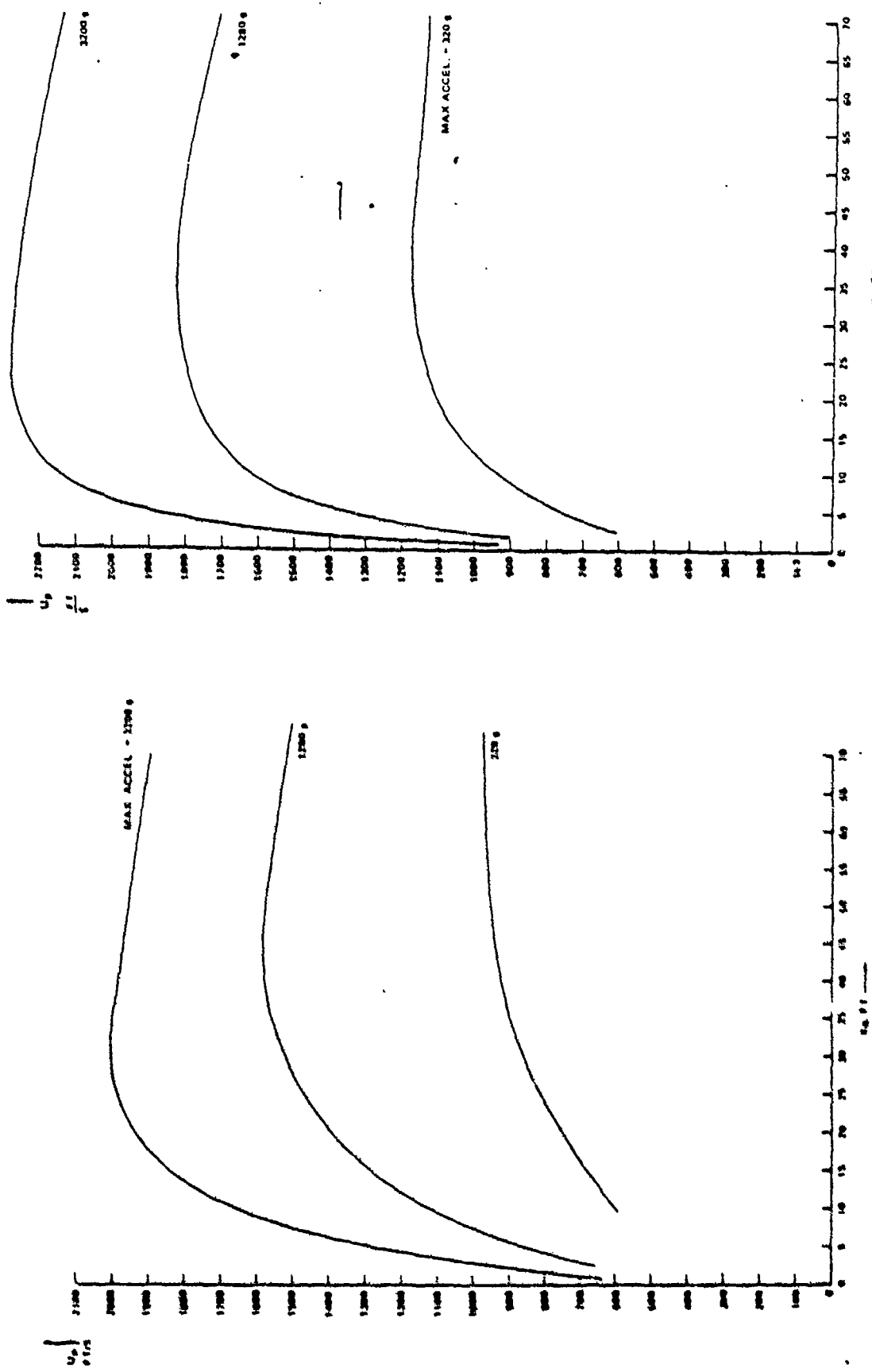


Figure 15. Velocity as Function of Breech Position for Fixed Length Air Gun  
Position for Fixed Length Air Gun

Figure 16. Velocity as Function of Breech Position  
for Fixed Length Air Gun,  $D_o/D_1 = 2$

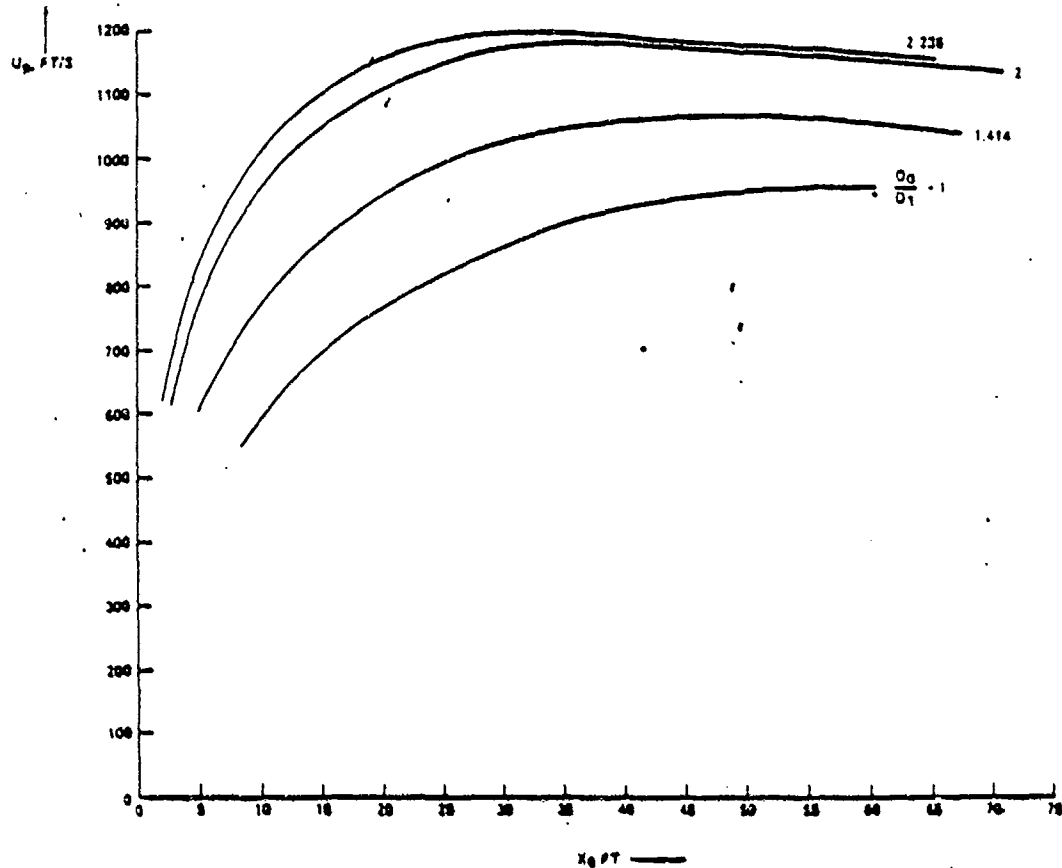


Figure 17. Velocity as Function of Breech Position for Fixed Length Air Gun, Max Acceleration = 320 g

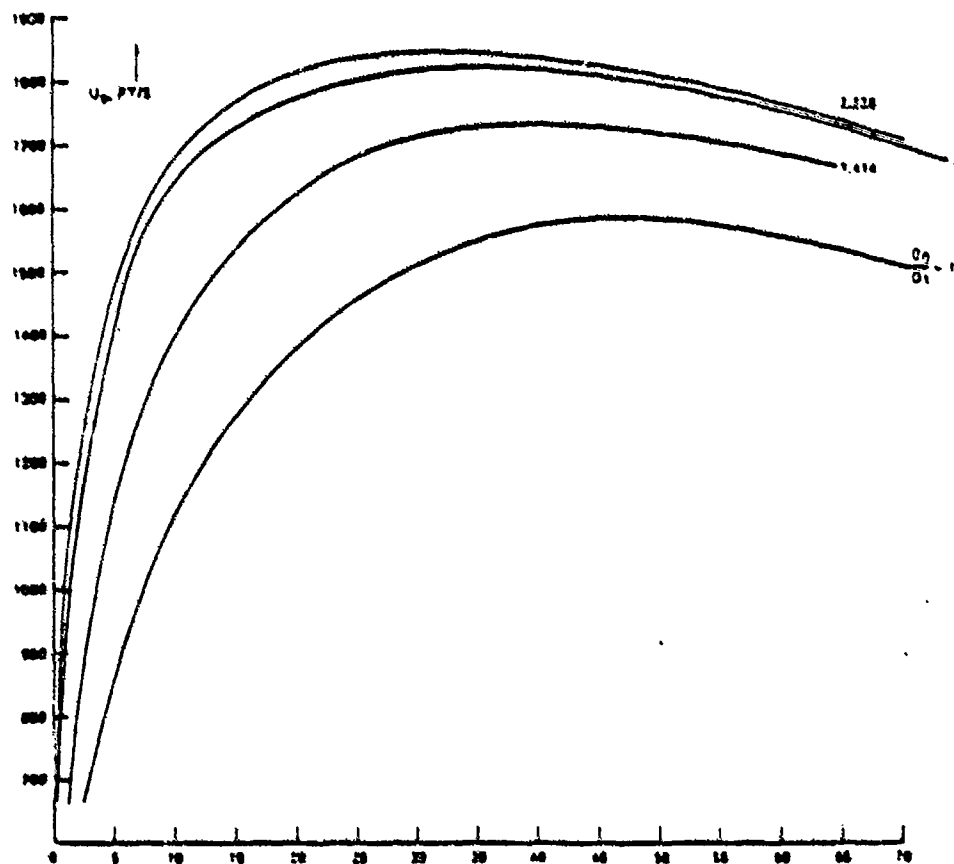


Figure 18. Velocity as Function of Breech Position for Fixed Length Air Gun, Max Acceleration = 1280 g

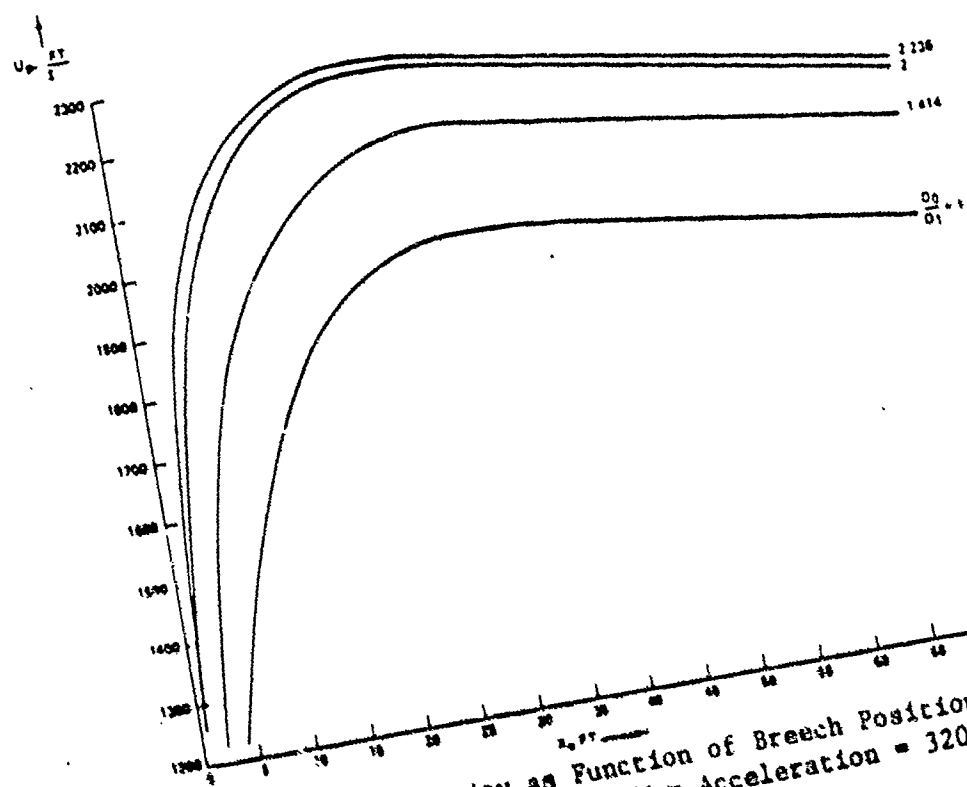


Figure 19. Velocity as Function of Breech Position for Fixed Length Air Gun, Max Acceleration = 3200 g

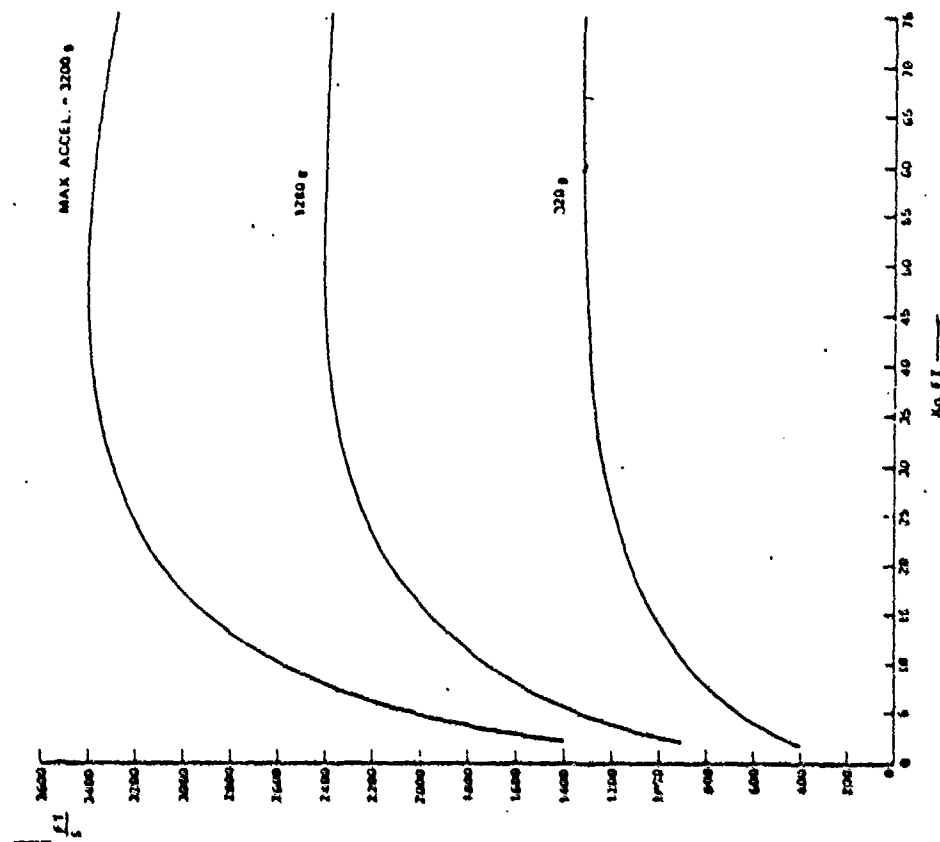


Figure 21. Velocity as Function of Breech Position for Fixed Length Helium Gun,  $D_o/D_1 = 2$

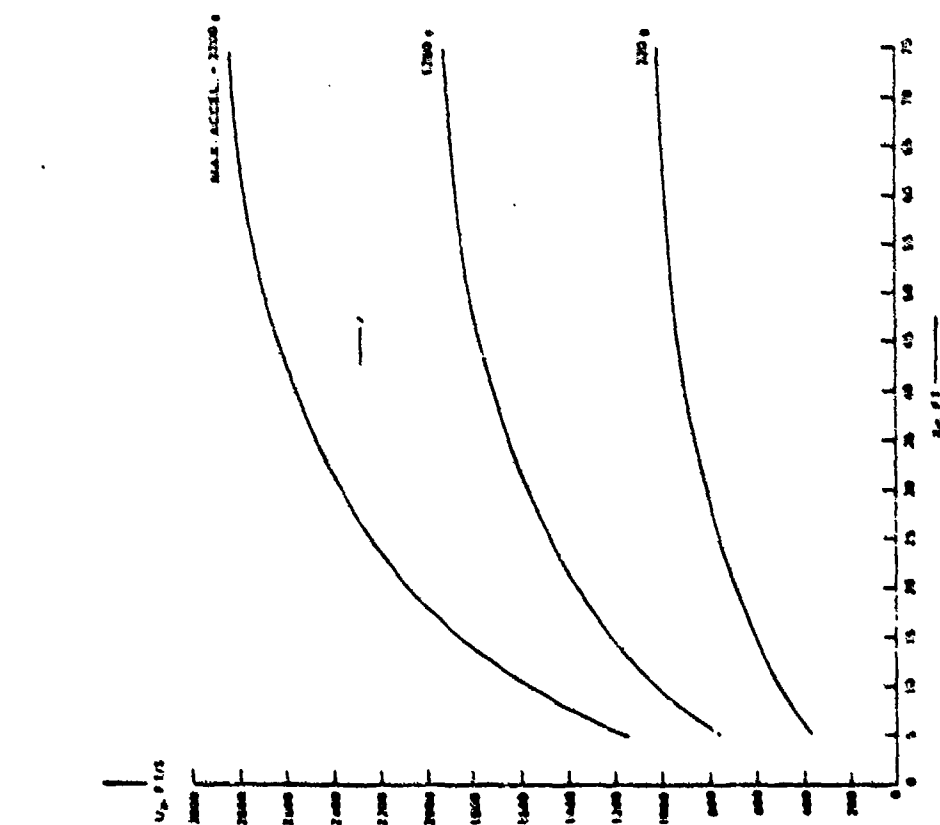


Figure 20. Velocity as Function of Breech Position for Fixed Length Helium Gun,  $D_o/D_1 = 1$

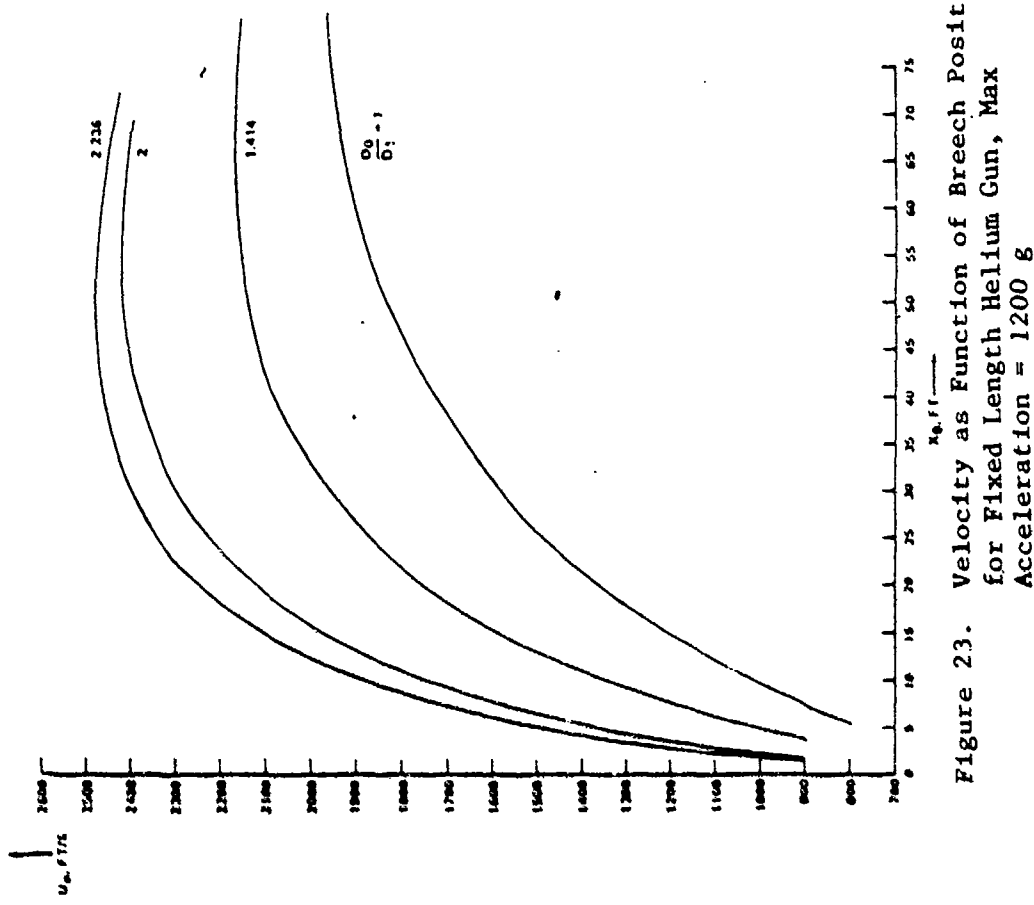


Figure 22. Velocity as Function of Breech Position  
for Fixed Length Helium Gun, Max  
Acceleration = 320 g

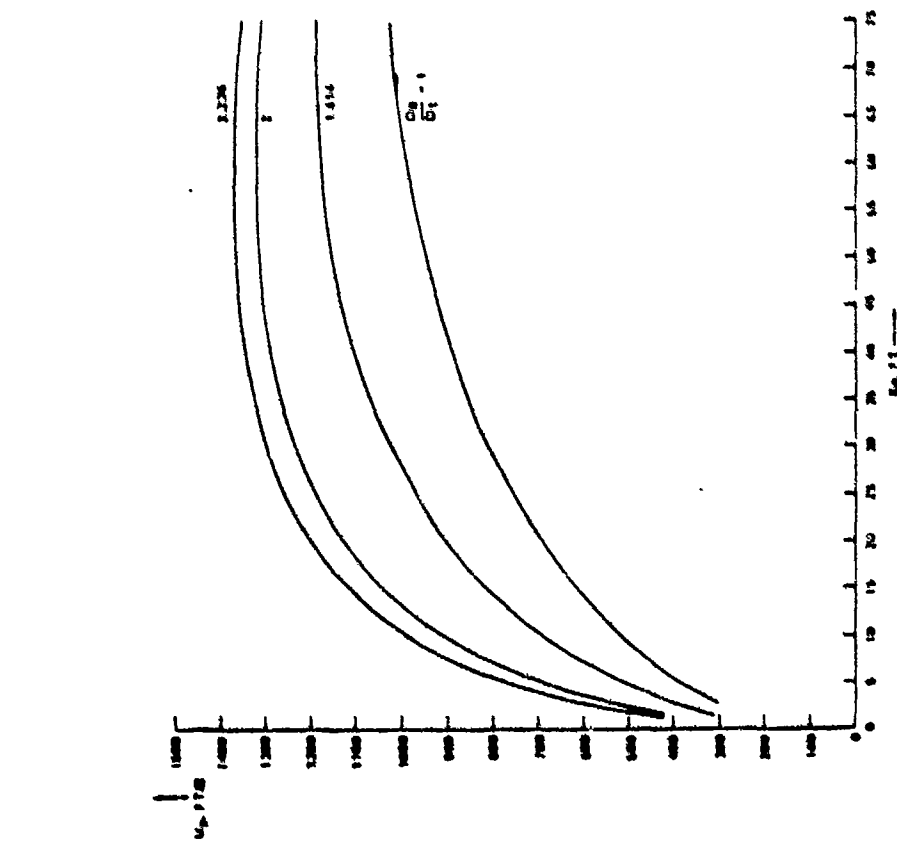


Figure 23. Velocity as Function of Breech Position  
for Fixed Length Helium Gun, Max  
Acceleration = 1200 g

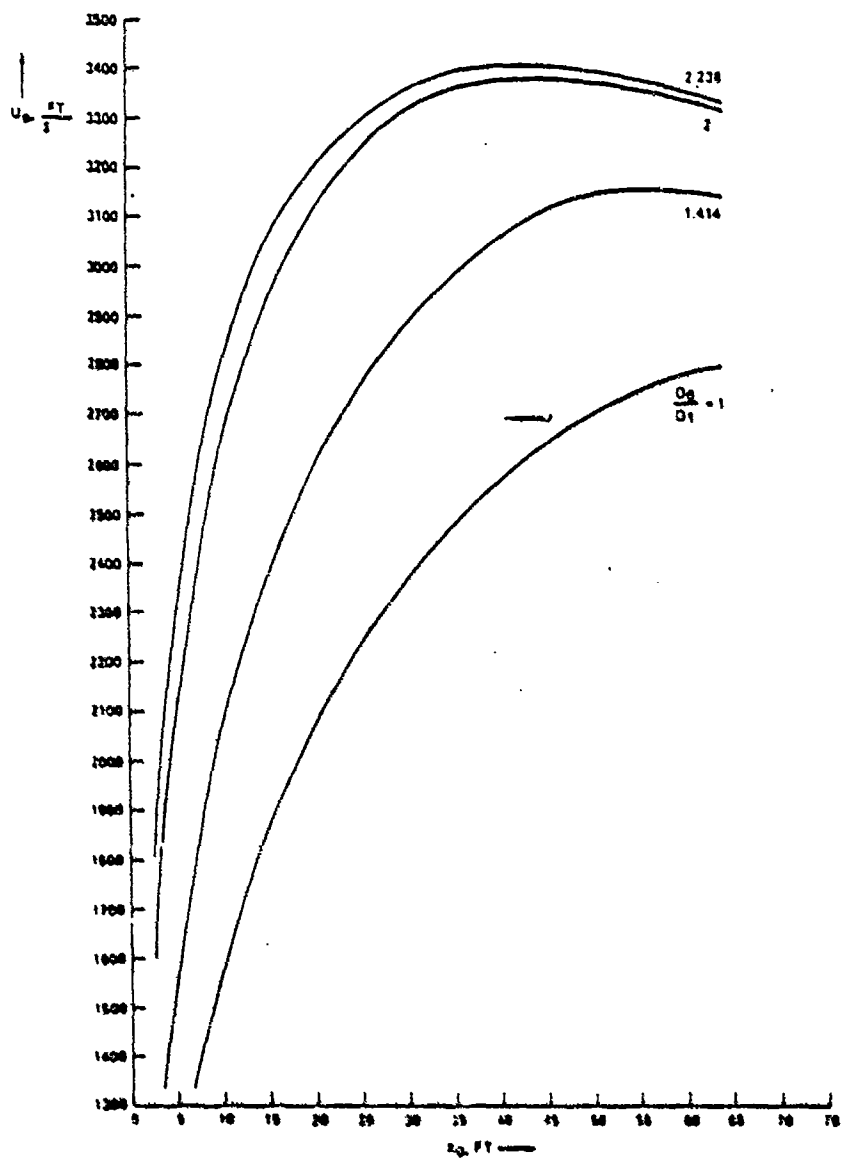


Figure 24. Velocity as Function of Breech Position  
for Fixed Length Helium Gun, Max  
Acceleration = 3200 g

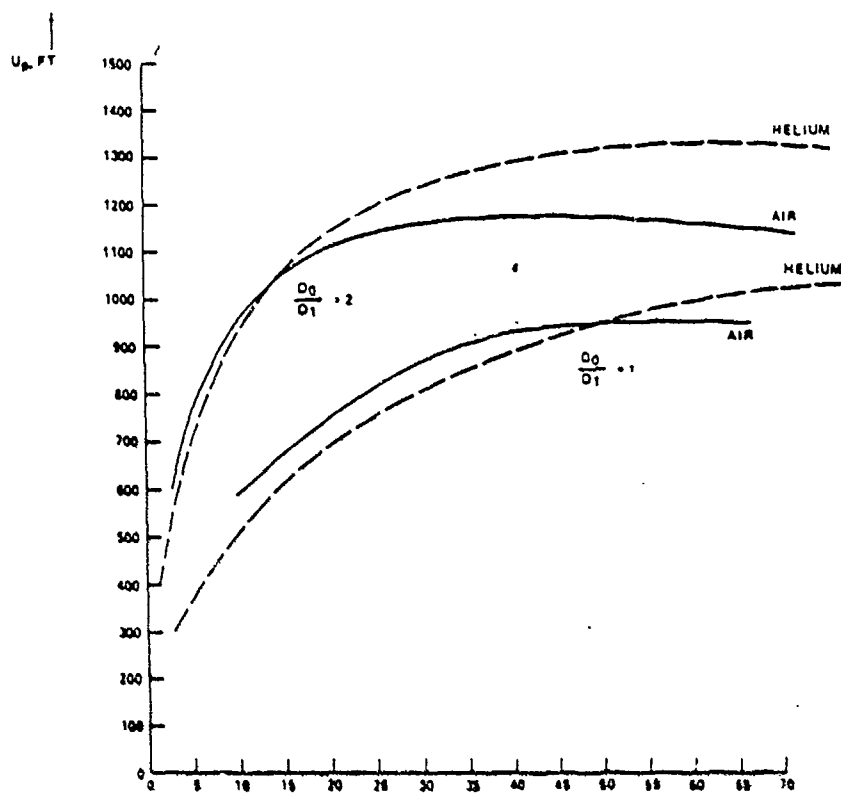


Figure 25. Velocity as Function of Breech Position  
for Fixed Length Gas Guns, Max Acceleration = 320 g

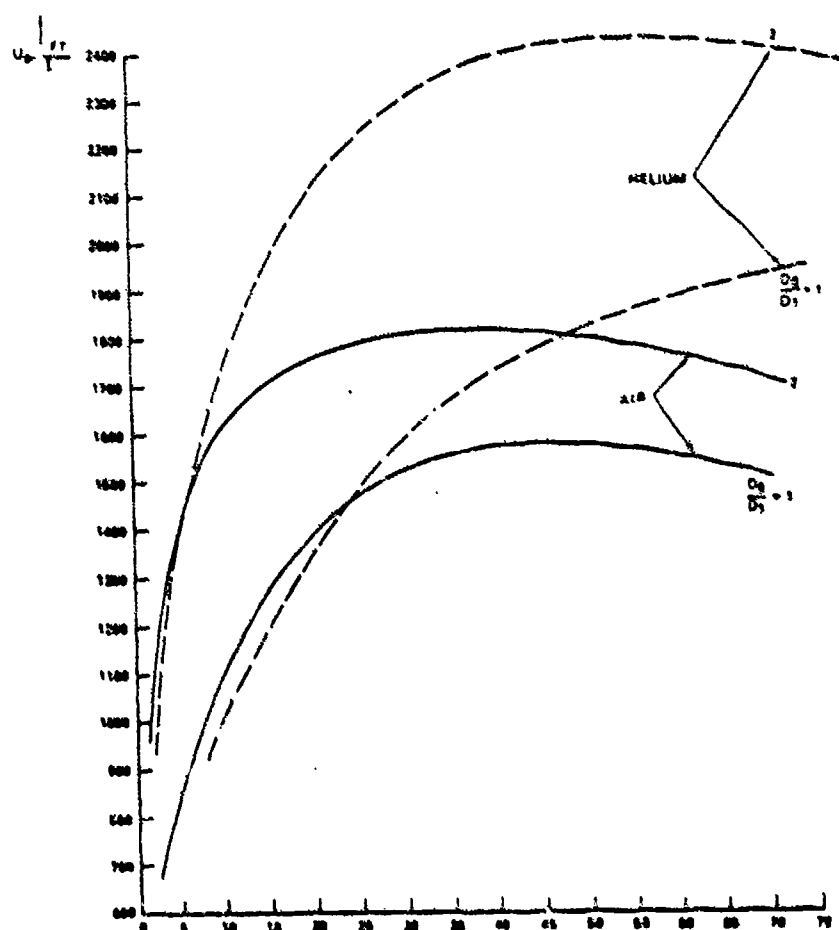


Figure 26. Velocity as Function of Breech Position for Fixed

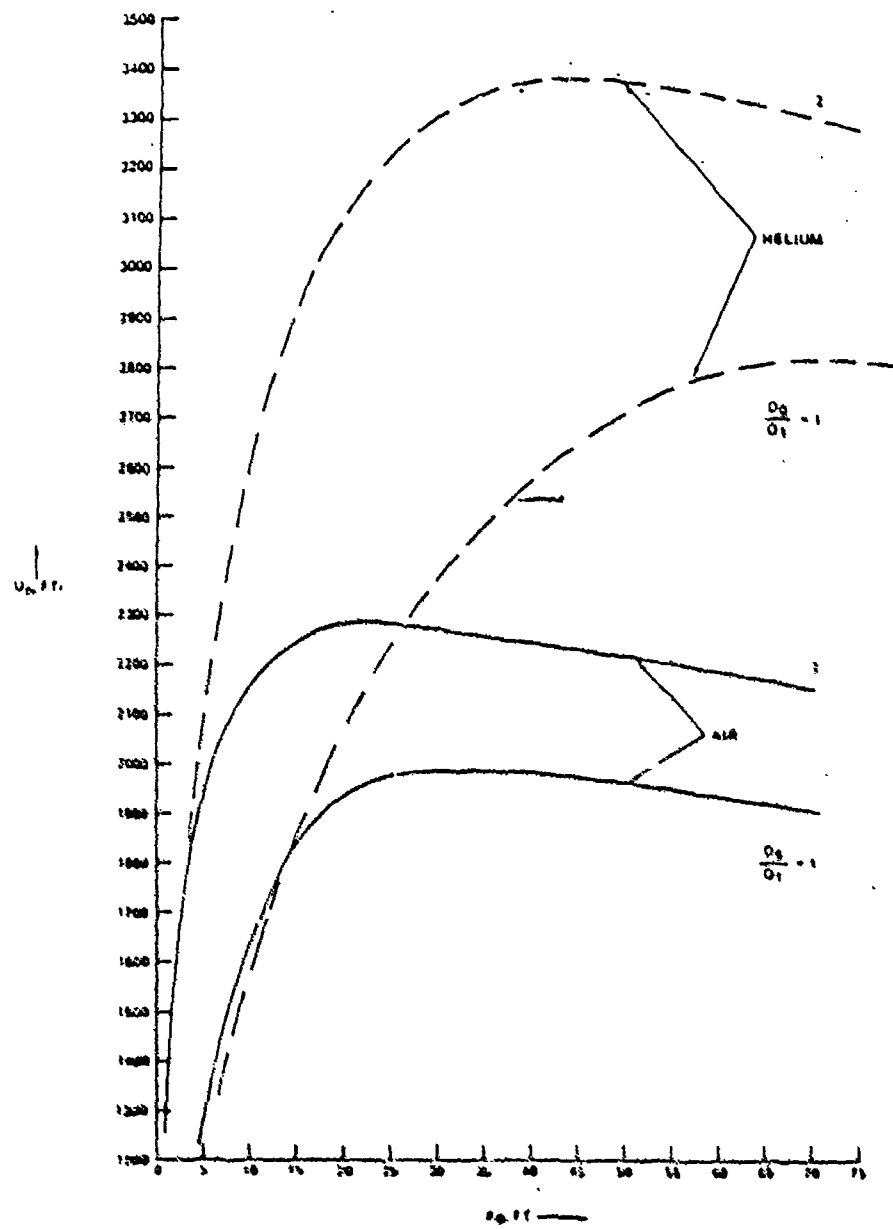


Figure 27. Velocity as Function of Breech Position  
for Fixed Length Gas Guns, Max  
Acceleration = 3200 g

(2) The compressed propellant gas expands isentropically. In fact, the gaseous friction effects and heat-transfer effects do decrease the projectile velocity. The quantitative decrease is a function of  $u_p/a_0$ , as has been shown.<sup>1</sup>

(3) Projectile friction is negligible. Whether or not this is true depends on the precision specified in fabrication of barrel and projectile as well as on the type of projectile material used.

(4) There is no gas leakage around the projectile. Again, this depends on the projectile and barrel construction, materials, and seals.

(5) The pressure in front of the projectile is negligible. This may be assured by evacuating the barrel.

Depending on the above effects in the region of velocities of the HDL gas guns, the experimental velocities will range from 2 to 12 percent of the calculated theoretical velocities.

---

<sup>1</sup>A. E. Seigel, The Theory of High Speed Guns, Agardograph 91 (May 1965), obtainable from the National Technical Information Service, Defense Documentation Center Springfield, VA, AD 475660.

## APPENDIX A.--DESCRIPTION OF THE PREBURNED PROPELLANT GUN

Here is described the gun system in which the propellant has been completely reacted before the projectile is allowed to move. This gun system is termed a preburned propellant (PP) gun. The gun consists of a chamber of diameter  $D_0$  joined by means of a transition section to a barrel of diameter  $D_1$ . The projectile is positioned initially so that its back end is at the beginning of the barrel section. Immediately before the projectile begins to move, the reacted propellant produces a gas in the chamber at an initial and peak pressure,  $P_0$ ; sound speed,  $a_0$ ; temperature,  $T_0$ , etc. (See fig. A-1.) (In the case of Harry Diamond Laboratories (HDL) guns, the zero subscript values are the initial conditions of the compressed gas).

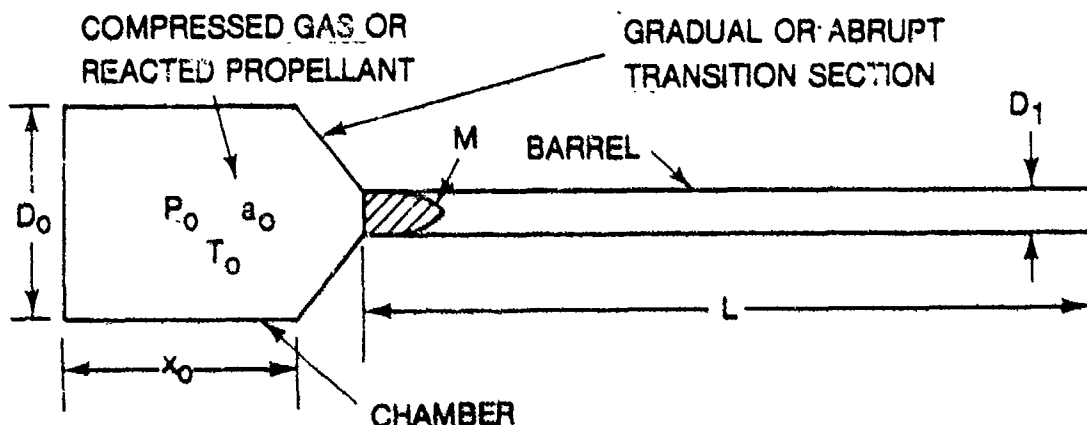


Figure A-1. HDL Preburned Propellant Gas Gun

When the chamber diameter is greater than the barrel diameter ( $D_0/D_1 > 1$ ), the gun is described as a "chambered" gun, or a gun with "chambrage." When the chamber diameter is equal to that at the barrel, the gun is described as "having no chambrage," or as a "constant diameter gun."

In practice, a PP gun may employ a diaphragm to separate the propellant in the chamber from the projectile; this diaphragm is ruptured when the propellant has completed its reaction. Another possibility is the use of a "shear disc" around the projectile itself: the disc shears when the reaction has been completed. The HDL PP gun uses as a propellant a nonreacting gas (such as compressed helium or air). A retractable pin restrains the projectile.

In a PP gun, the projectile is restricted from movement until the pressure has reached a peak value; it can be shown that, after the projectile is released, the pressure behind the projectile decreases as the projectile increases in velocity and moves along the barrel. (See fig. A-2).

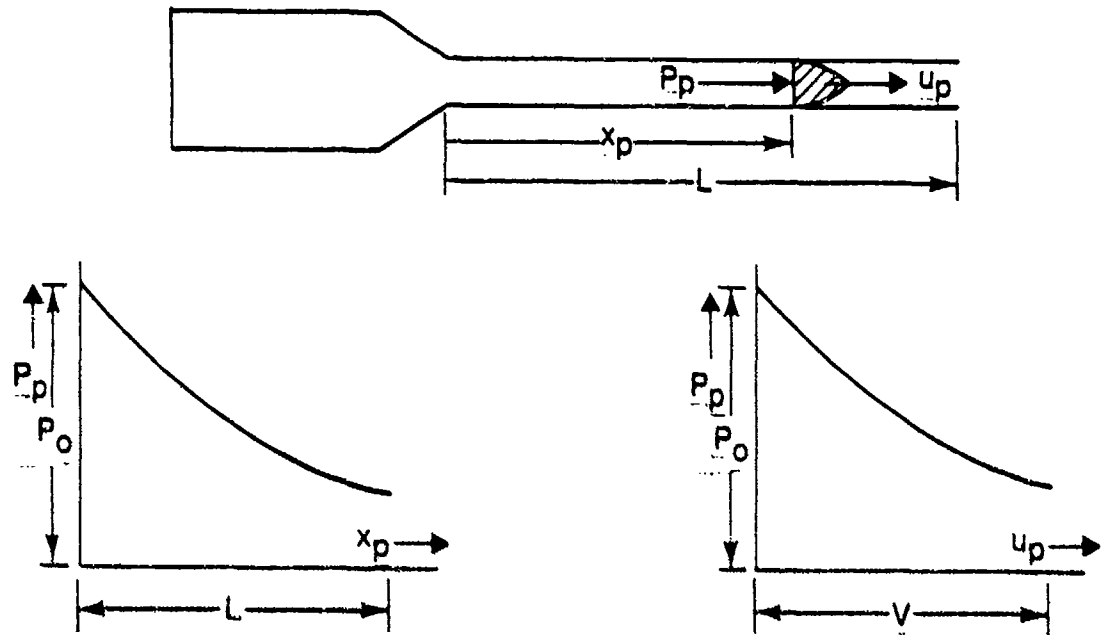


Figure A-2. Pressure versus Velocity in Gun Barrel.

APPENDIX B.—THE GAS DYNAMICS EQUATIONS FOR A CHAMBERED PROPELLANT GAS GUN

To determine analytically the behavior of the expanding propellant gas in a chambered gun, the assumption is made that the flow is isentropic.

The one-dimensional characteristic equations are applicable to the constant diameter chamber and are applicable to the constant diameter barrel:

$$\frac{\partial}{\partial t} (u \pm \sigma) + (u \pm a) \frac{\partial}{\partial x} (u \pm \sigma) = 0,$$

where the sound speed,  $a$ , and the Riemann function,  $\sigma$ , are defined by

$$a^2 \equiv \left( \frac{\partial p}{\partial \rho} \right)_s,$$

$$d\sigma \equiv (dp/a\rho)_s.$$

With the notation

$$\frac{D}{Dt} \equiv \frac{\partial}{\partial t} + (u \pm a) \frac{\partial}{\partial x},$$

the characteristic equations become

$$\frac{D(u \pm \sigma)}{Dt} = 0 \quad (B-1)$$

(See fig. B-1).

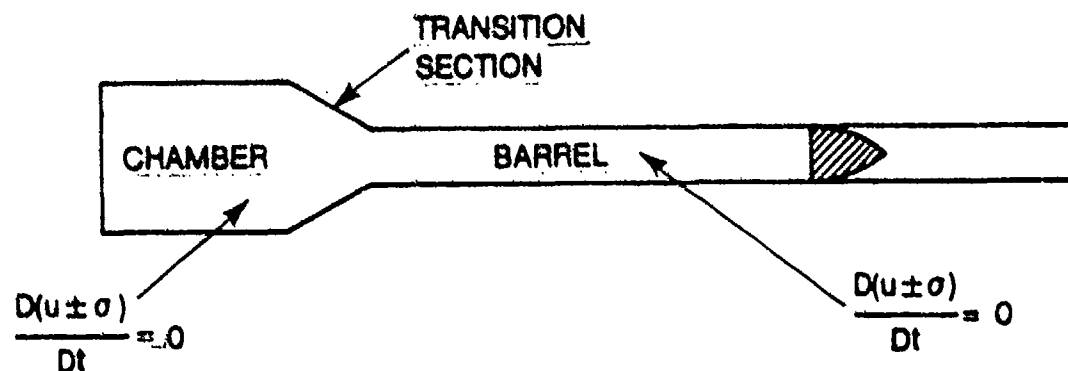


Figure B-1. Gas Dynamics for Chambered Propellant Gas Gun

The gas flow in the transition section, which joins the chamber to the bore, is actually a two-dimensional unsteady flow. However, it is not feasible to solve the two-dimensional unsteady equations. There are two possible approximate methods of treating the flow through the transition section. The first method is to assume that the change in area from the chamber to the barrel occurs gradually so that the flow may be assumed to be one-dimensional. Then, the one-dimensional characteristic method can be applied to this change in area section. The characteristic equations become, for the change in area section,

$$\frac{D(u \pm \sigma)}{Dt} = \frac{\partial}{\partial t} (u \pm \sigma) + (u \pm a) \frac{\partial}{\partial x} (u \pm \sigma) = \pm \frac{au}{A} \frac{dA}{dx}, \quad (B-2)$$

where  $u$  is the gas velocity,  $a$  is the sound speed,  $\sigma$  is the Riemann function, and  $A$  is the cross-sectional area of the gas layer at position  $x$  in time  $t$ . These equations require a tedious numerical procedure to solve and are generally not suitable for hand computation. However, the quantity  $u \pm \sigma$ , in contrast to the constant diameter case, does not remain constant for disturbances in the transition section.

The second approach, one chosen here as being more convenient and a good approximation to the actual situation, is to assume the following: At any given time, the rate of change of mass and energy within the transition section is negligible relative to the differences between the exit and entrance fluxes of these quantities; thus, the changes due to variations of time are assumed negligible relative to those due to the variations in position within the control volume. This assumption is made clear by taking as a control volume the transition section as shown in figure B-2.

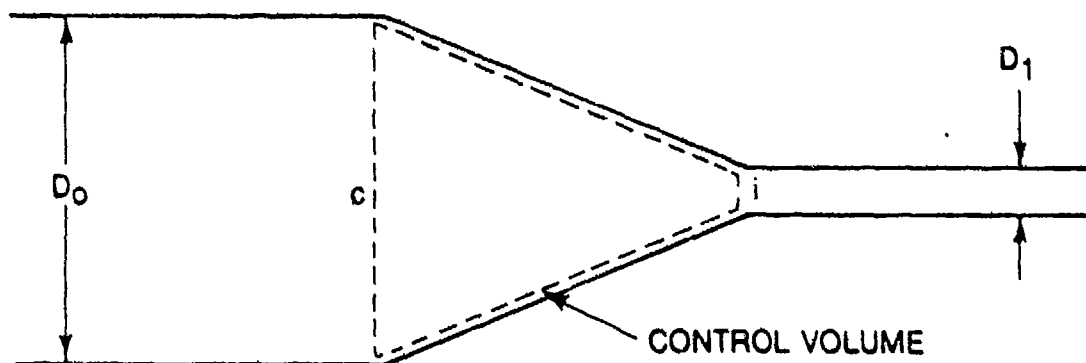


Figure B-2. Variations of Time, Mass, and Energy.

Then the applicable equations of continuity and energy are, respectively,

$$\left( \frac{\partial m}{\partial t} \right)_{\text{ConVol}} = (\rho u A)_c - (\rho u A)_i \quad (B-3)$$

and

$$\left( \frac{\partial E}{\partial t} \right)_{\text{ConVol}} = \left[ \left( h + \frac{u^2}{2} \right) (\rho u A) \right]_c - \left[ \left( h + \frac{u^2}{2} \right) (\rho u A) \right]_i, \quad (B-4)$$

where  $m$  and  $E$  are the mass and the internal energy in the transition section. By our assumption above, the two unsteady terms on the left side of equations (B-3) and (B-4) are negligible.

It is observed that, if the transition is rather sudden, the control volume is small; hence, since the unsteady terms on the left side of these equations are proportional to the magnitude of the control volume, the unsteady terms are necessarily small. Thus, in the case of a sudden transition, the assumption above is automatically valid.

With this assumption, the equations which are applicable to relate the conditions at the entrance of a transition section to those at the exit of the transition section are the quasi-steady equations of continuity and energy. Thus, at each instant of time, the applicable equations are

$$h_c + \frac{u_c^2}{2} = h_i + \frac{u_i^2}{} = \text{function of time}, \quad (B-5)$$

$$\rho_c u_c A_c = \rho_i u_i A_i = \text{function of time}. \quad (B-6)$$

Since the flow has been assumed isentropic, the thermodynamic relation between enthalpy and pressure is

$$dh = (dp/\rho)_s \quad (B-7)$$

and

$$h_i - h_c = \int_{p_c}^{p_i} \frac{dp}{\rho} \quad (B-8)$$

Equation (5) becomes

$$\frac{u_i^2 - u_c^2}{2} = \int_{p_i}^{p_c} \frac{dp}{\rho}. \quad (B-9)$$

It may be shown from equations (B-3) and (B-4) that the use of the quasi-steady flow equations to describe the gas flow between the chamber and the barrel of the gun yields a larger projectile velocity than would be yielded by the use of the actually applicable unsteady equations. However, experimental results from a chambered PP gun by Seigel and Dawson have demonstrated that the difference was small enough to be unmeasurable. These experiments were made with a gun using room temperature air at about 3000 lb/in<sup>2</sup> as a propellant. The gun had a 0.50-in.-diameter barrel, which could be joined to various chambers of 30-deg half-angle taper. The projectiles were 1-gm plastic projectiles and were sheared by the compressed air in the chamber. The measured projectile velocities were compared with the theoretically predicted velocities based on the use of the quasi-steady equations above.

The comparison showed that the quasi-steady flow approximation in the transition section yields good agreement with experiment.

Figure B-3 diagrams the characteristics of a chambered PP gun in action.

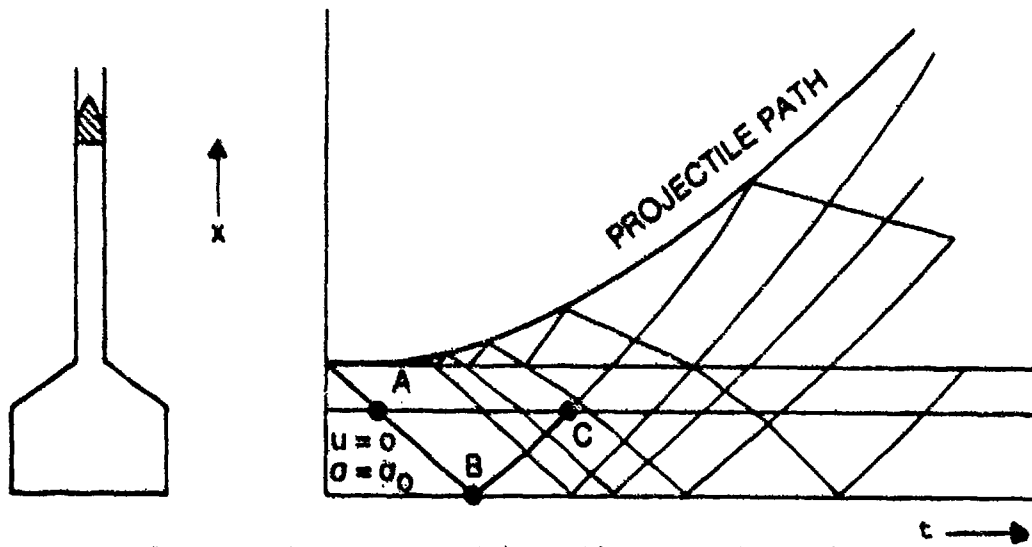


Figure B-3. Preburned Propellant Gun in Action.

Characteristics may be drawn in the transition section by fairing them from the known conditions at the inlet to the known conditions at the exit. The simple wave region in the chamber for which  $u + \sigma = \sigma_0$  is denoted by the letters A, B, and C.

With equations (B-1), (B-6), and (B-8) and the isentropic equations of state of the gas, it is possible to calculate quantitatively the behavior of the projectile in a PP chambered gun.

For the HDL gas guns, the ideal equation of state was used:

$$p = \rho RT, \quad (B-10)$$

$$p = \rho^Y p_0 / \rho_0^Y. \quad (B-11)$$

From these equations, the sound speed and the Riemann function become

$$a^2 = \gamma p / \rho = \gamma RT, \quad (B-12)$$

$$\sigma = 2a / (\gamma - 1), \quad (B-13)$$

where  $\sigma$  is taken to be zero at  $a = 0$ . The enthalpy for an ideal gas is

$$h = a^2 / (\gamma - 1) = (\gamma - 1) \sigma^2 / 4. \quad (B-14)$$

## APPENDIX C.--CALCULATIONS BY ELECTRONIC COMPUTING MACHINES

The method of characteristics as outlined in Appendix B may be numerically applied to calculate the performance of a preburned propellant (PP) gun system. However, in the cases where the chamber is not effectively infinite in length, hand calculation becomes extremely lengthy and tedious. Further, the accuracy of the calculated results depends on the spacing of the numerical points. The greater the spacing, the greater the error; hand calculation, particularly, does not allow small spacing. Thus, calculating by electronic computing machines offers great advantages compared with hand calculation. Not only is much time saved, but accuracy may be substantially increased.

Calculations have been obtained by electronic computing machines. The results may be expressed in terms of dimensionless plots of  $u_p$  versus  $\bar{x}_p$ , or they may be in terms of other dimensionless variables. Thus, a plot of dimensionless projectile velocity versus projectile travel for a given geometry (i.e., for a given  $D_0/D_1$  and a given  $G/M$ ) has been found convenient. The results of computations made for the U.S. Naval Ordnance Laboratory at the Naval Weapons Laboratory on electronic computing machines have been published for a PP ideal gas gun.<sup>1</sup> The plots in figure C-1 present curves of  $u_p/a_0$  versus  $\bar{x}_p$  for varying values of  $G/M$  and a given  $D_0/D_1$  and  $\gamma$  (as adapted from Agardograph 91, fig. 20<sup>1</sup>).

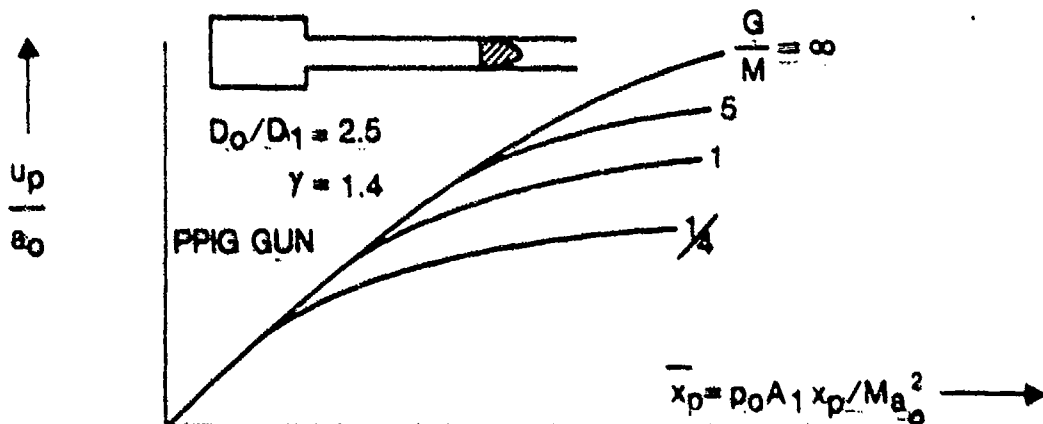


Figure C-1. Curves for Preburned Propellant Ideal Gas Gun Behavior.

<sup>1</sup> A. E. Seigel, The Theory of High Speed Guns, Agardograph 91 (May 1965), fig. 20 and 21, obtainable from the National Technical Information Service, Defense Documentation Center, Springfield, VA, AD 475660.

The curve marked  $G/M = \infty$  is the infinite chamber length case.

The above curves are replotted in figure C-2 as  $u_p/a_0$  versus  $P_0 A_1 x_p/M a_0^2$  for varying values of  $D_0/D_1$  and a given  $G/M$  and  $\gamma$  (as adapted from Agardograph 91, fig. 21<sup>1</sup>).

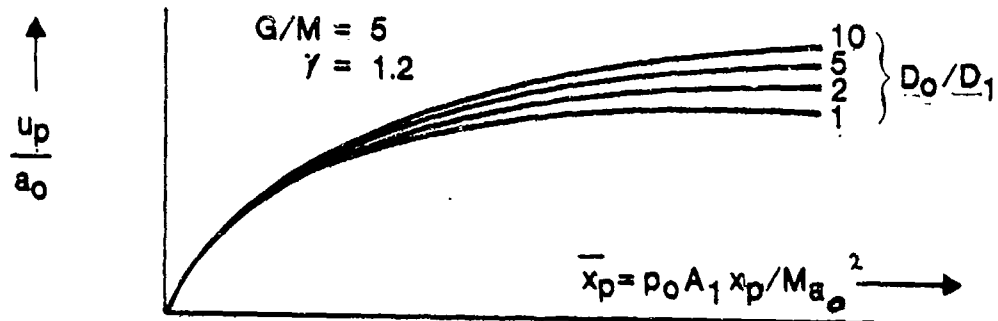


Figure C-2. Replotted Curves for Preburned Propellant Ideal Gas Gun Behavior.

Figures 20 and 21 of Agardograph 91<sup>1</sup> thus present the entire performance of a projectile in a PP ideal gas gun with chambrage (chamber).

<sup>1</sup> A. E. Seigel, The Theory of High Speed Guns, Agardograph 91 (May 1965), fig. 20 and 21, obtainable from the National Technical Information Service, Defense Documentation Center, Springfield, VA, AD 475660.

#### APPENDIX D.--THE SPECIAL SOLUTION OF PIDDUCK-KENT

The classical LaGrange Problem of Internal Ballistics presents the situation where a projectile initially at rest in a constant cross-sectional area gun is propelled by a propellant which burns instantaneously. This is the problem of the preburned propellant (PP) gun. The process is considered to be one-dimensional, frictionless, and adiabatic. LaGrange initiated the study of this problem in 1793 when he presented an approximate solution to the problem. After LaGrange had initiated the study of the LaGrange Problem, Hugoniot extended Riemann's theory of waves of finite amplitude and applied it to the problem; he solved it to the point where the first expansion disturbance shed by the projectile reached the breech. Gossot and Louisville went still further and followed the first expansion disturbance after it had been reflected from the breech back to the projectile. The culmination of this method of attack (which did not use the method of characteristics) was the complete solution by Love in 1921 up to the first disturbance traveling back and toward the breech for the third time.

Love replaced the system of hyperbolic quasi-linear partial differential equations, which describe the problem by a single partial differential equation of second order, for one single dependent variable and solved it separately for each wavelet. His solution contained lengthy and involved computations and was valid only for a Noble-Abel gas (with isentropic relation  $p(v - b)^\gamma = \text{constant}$ ), whose ratio of specific heats was of the form

$$\gamma = \frac{2n+1}{2n-1},$$

where  $n$  is an integer.

Pidduck noted, from the results he had calculated with Love's equations, that the ratio of the breech pressure to the pressure of the gas directly behind the projectile oscillated as shown in figure D-1.

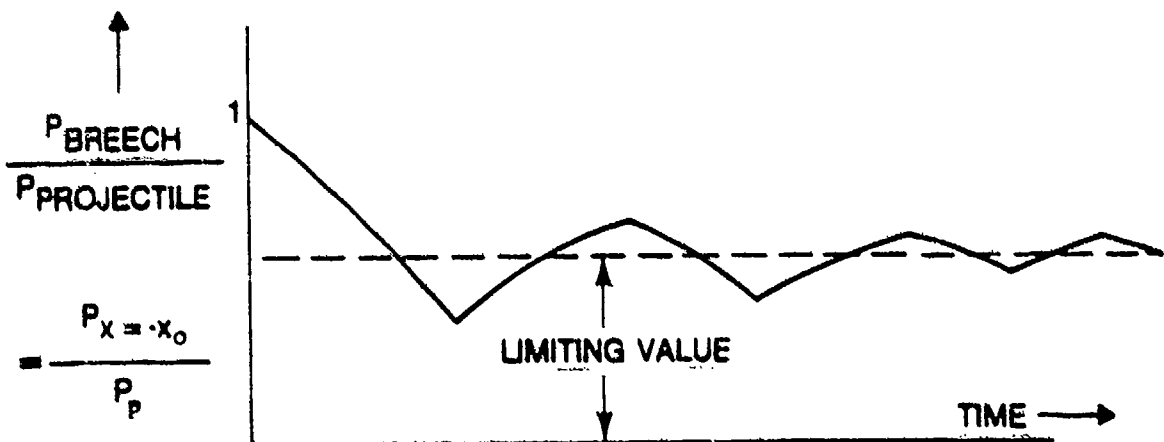


Figure D-1. Oscillation of Frictionless Gun.

This oscillation results from the lowering of the pressure occurring as the first disturbance reflects back and forth between breech and projectile. Pidduck found that the oscillations damped out and that the pressure ratio approached a certain limiting value. He then deduced a "special solution" to the governing differential equations which indeed did yield the condition that the ratio  $P_{(x=x_0)}/P_p$  is a constant, not only in a limit but at all times. This solution, an analytic one, did not satisfy the initial conditions of the LaGrange Problem; the initial conditions for the special solution were a nonuniform distribution of density and pressure. Pidduck and all later investigators have suspected, but not proved, that the accurate solution to the LaGrange Problem approached the special solution in the limit of large travel.

The special solution has also been derived by Kent and by Vinti and Kravitz (see also Corner). It is often referred to as "The Pidduck-Kent Special Solution" or "Pidduck Special Solution." The essential results are

$$\frac{u}{u_p} = \frac{x + x_0}{x_p + x_0}, \quad (D-1)$$

$$\frac{P_{x=x_0}}{P_p} = (1 - a_0)^{-\gamma/(\gamma-1)}, \quad (D-2)$$

or, for a  $\gamma = 1$  gas,

$$\frac{P_{x=x_0}}{P_p} = e^{a_0}, \quad (D-3)$$

where  $a_0$  and  $a_0$  depend on  $G/M$  and  $\gamma$ , as shown below and plotted in figure D-2.

$$\frac{G}{M} = \frac{2\gamma}{\gamma - 1} a_0 (1 - a_0)^{-\gamma/(\gamma-1)} \int_0^1 (1 - a_0 \mu^2)^{1/(\gamma-1)} d\mu. \quad (D-4)$$

Or, for a  $\gamma = 1$  gas,

$$\frac{G}{M} = 2a_0 e^{a_0} \int_0^1 e^{-a_0 \mu^2} d\mu. \quad (D-5)$$

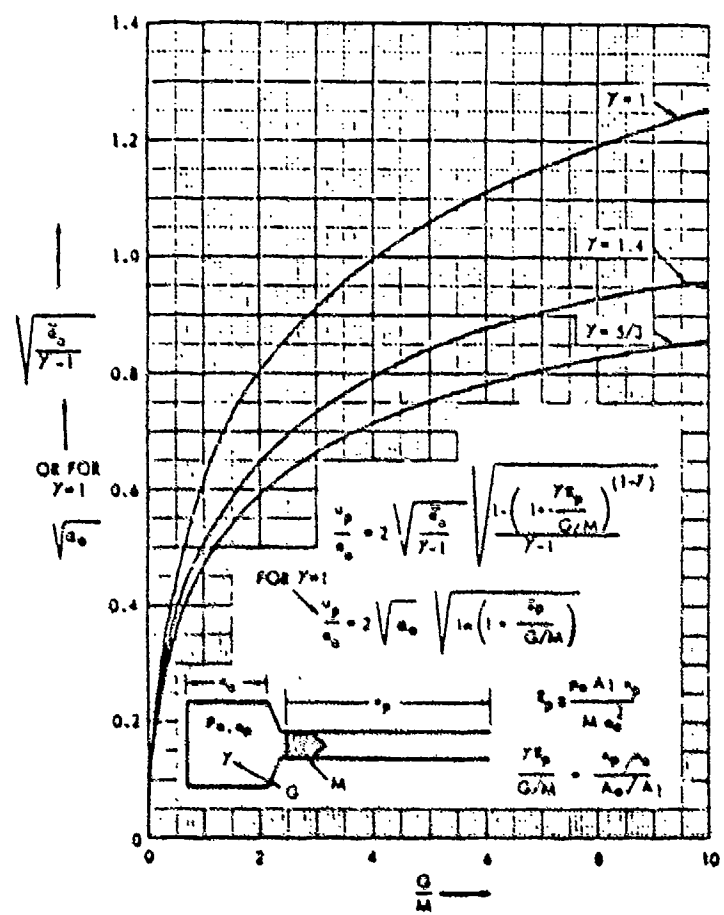


Figure D-2. Pidduck-Kent Special Solution.

For small  $G/M$ ,  $\tilde{a}_0$  may be approximated as

$$a_0 = \frac{G(\gamma - 1)}{M(2\gamma)} \left\{ 1 - \frac{3\gamma - 1}{6\gamma} \frac{G}{M} + \left[ \frac{1}{4} - \frac{1}{12\gamma} + \frac{1}{180\gamma^2} \right] \left( \frac{G}{M} \right)^2 + \dots \right\} . \quad (D-6)$$

The projectile velocity is obtained as

$$u_p = \frac{2a_0 \sqrt{\tilde{a}_0}}{\gamma - 1} \left[ 1 - \left( \frac{x_0}{x_p + x_0} \right)^{\gamma-1} \right]^{1/2}$$

$$= \frac{2a_0 \sqrt{a_0}}{\gamma - 1} \left[ 1 - \left( 1 + \frac{\gamma x_p}{G/M} \right)^{1-\gamma} \right]^{1/2}$$

and, for  $\gamma = 1$ ,

$$u_p = 2a_0 \sqrt{a_0} \left( \log_e \frac{x_p + x_0}{x_0} \right)^{1/2}$$

$$= 2a_0 \sqrt{a_0} \left[ \log_e \left( 1 + \frac{\bar{x}_p}{G/M} \right) \right]^{1/2} , \quad (D-8)$$

where

$$\bar{x}_p = \frac{P_0 A_1 x_p}{M a_0^2} . \quad (D-9)$$

Thus, figure D-2 may be used with equations (D-7) to (D-9) to calculate the projectile velocity for any gun, even a chambered gun, although the solution was derived for a  $D_0/D_1 = 1$  gun. Then, for the chambered gun,  $x_0$  should be replaced by  $x_0 A_0 / A_1$  in equations (D-7) and (D-8).

The above results may be deduced for a  $D_0/D_1 = 1$  gun with a covolume propellant gas, and these results have been applied as an approximation even to the case of a chambered gun with a covolume propellant gas. In the chambered covolume case, the sound velocity,  $a_0$ , in all the equations above should be replaced by  $\sqrt{\gamma RT_0} = \sqrt{\gamma P_0 / (v_0 - b)}$  and  $x_0$  should be replaced by  $(A_0 x_0 - bG) / A_1$ .

It is found that, when  $G/M$  becomes infinite,  $\tilde{a}_0$  approaches 1. In this case, for the  $D_0/D_1 = 1$  gun, the projectile velocity becomes, from equation (D-7),

$$u_p = \frac{2a_0}{\gamma - 1} \left[ 1 - \left( \frac{x_0}{x_p + x_0} \right)^{\gamma-1} \right]^{1/2}, \quad (D-10)$$

which, for infinite travel distance, becomes equal to  $2a_0/(\gamma - 1)$ ; this is, as it should be, the escape velocity for a  $D_0/D_1 = 1$ ,  $x_0 = \infty$  gun.

The special solution applies to the  $D_0/D_1 = 1$  gun in which, initially, there is a pressure gradient in the propellant gas; the LaGrange ballistics problem (the PP gun), however, assumes no gradients initially. Pidduck and later investigators suspected, but never proved, that the special solution approaches the accurate solution in the limit of large travel. The results of calculations made on the electronic computing machines seem to confirm their suspicion.

The computed results indicate that, indeed, the special solution is an amazingly good approximation for the finite chamber length PP gun for any  $D_0/D_1$ ; this is particularly true for  $G/M$  values less than  $1/4$ .

DISTRIBUTION

ADMINISTRATOR  
DEFENSE TECHNICAL INFORMATION CENTER  
ATTN DTIC-DDA (12 COPIES)  
CAMERON STATION, BUILDING 5  
ALEXANDRIA, VA 22314

COMMANDER  
US ARMY RSCH & STD GP (EUR)  
ATTN CHIEF, PHYSICS & MATH BRANCH  
FPO NEW YORK 09510

COMMANDER  
US ARMY MISSILE & MUNITIONS CENTER  
& SCHOOL  
ATTN ATSK-CTD-F  
REDSTONE ARSENAL, AL 35809

DIRECTOR  
US ARMY BALLISTIC RESEARCH LABORATORY  
ATTN DRDAR-TSB-S (STINFO)  
ABERDEEN PROVING GROUND, MD 21005

ENGINEERING SOCIETIES LIBRARY  
345 EAST 47th STREET  
ATTN ACQUISITIONS DEPARTMENT  
NEW YORK, NY 10017

US ARMY ELECTRONICS RESEARCH &  
DEVELOPMENT COMMAND  
ATTN TECHNICAL DIRECTOR, URDEL-CT

HARRY DIAMOND LABORATORIES  
ATTN CO/TD/TSO/DIVISION DIRECTORS  
ATTN RECORD COPY, 81200  
ATTN HDL LIBRARY, 81100 (3 COPIES)  
ATTN HDL LIBRARY, 81100 (WOODBRIDGE)  
ATTN TECHNICAL REPORTS BRANCH, 81300  
ATTN CHAIRMAN, EDITORIAL COMMITTEE  
ATTN LEGAL OFFICE, 97000

DEPARTMENT OF COMMERCE  
NATIONAL BUREAU OF STANDARDS  
ATTN LIBRARY  
WASHINGTON, DC 20234

DIRECTOR  
DEFENSE ADVANCED RESEARCH PROJECTS AGENCY  
ARCHITECT BLDG  
1400 WILSON BLVD  
ATTN MATERIALS SCIENCES  
ATTN ADVANCED CONCEPTS DIV  
ATTN TARGET ACQUISITION & ENGAGEMENT DIV  
ATTN WEAPONS TECH & CONCEPTS DIV  
ARLINGTON, VA 22209

COMMANDER  
US ARMY ARMAMENT RESEARCH AND DEVELOPMENT  
COMMAND  
ATTN DRDAR-TS, TECHNICAL SUPPORT DIV  
DOVER, NJ 07801

COMMANDER  
US ARMY MATERIALS AND MECHANICS RESEARCH  
CENTER  
ATTN DRXMR-PL, TECHNICAL LIBRARY  
ATTN DRXMR-T, MECHANICS AND ENGINEERING  
LABORATORY  
WATERTOWN, MA 02172

ARMY RESEARCH OFFICE (DURHAM)  
ATTN DRXRO-EG, DIR ENGINEERING DIV  
P.O. BOX 12211  
RESERACH TRIANGLE PARK, NC 27709

SUPERINTENDANT  
NAVAL POSTGRADUATE SCHOOL  
ATTN LIBRARY, CODE 2124  
MONTEREY, CA 93940

DIRECTOR  
NAVAL RESEARCH LABORATORY  
ATTN 2600, TECHNICAL INFO DIV  
WASHINGTON, DC 20375

COMMANDER  
NAVAL SURFACE WEAPONS CENTER  
ATTN E-40, TECHNICAL LIB  
WHITE OAK, MD 20910

DEPUTY CHIEF OF STAFF  
RESEARCH AND DEVELOPMENT  
HEADQUARTERS, US AIR FORCE  
ATTN AFRDQSM  
WASHINGTON, DC 20330

AF AERO-PROPULSION LABORATORY  
WRIGHT-PATTERSON, AFB, OH 45433

COMMANDER  
ARNOLD ENGINEERING DEVELOPMENT CENTER  
ATTN DY, DIR TECHNOLOGY  
ARNOLD AIR FORCE STATION, TN 37389

SANDIA NATIONAL LABORATORIES  
P.O. BOX 5800  
ALBUQUERQUE, NM 87185

CIVIL ENGINEERING RESEARCH FACILITY  
UNIVERSITY OF NEW MEXICO  
P.O. BOX 198  
ALBUQUERQUE, NM 87131